

**COMPARATIVE EVALUATION OF THE WEAR
RESISTANCE OF TWO DIFFERENT IMPLANT
ABUTMENT MATERIALS AFTER CYCLIC
LOADING – AN *IN VITRO* STUDY**

Dissertation Submitted to

THE TAMILNADU Dr. M.G.R. MEDICAL UNIVERSITY

In partial fulfillment for the Degree of

MASTER OF DENTAL SURGERY



**BRANCH I
PROSTHODONTICS AND CROWN & BRIDGE
MAY 2019**

**THE TAMILNADU Dr. M.G.R. MEDICAL UNIVERSITY
CHENNAI**

DECLARATION BY THE CANDIDATE

I hereby declare that this dissertation titled “**COMPARATIVE EVALUATION OF THE WEAR RESISTANCE OF TWO DIFFERENT IMPLANT ABUTMENT MATERIALS AFTER CYCLIC LOADING**” is a bonafide and genuine research work carried out by me under the guidance of **Dr.Vallabh Mahadevan, M.D.S.**, Reader, Department of Prosthodontics and Crown & Bridge, Ragas Dental College and Hospital, Chennai.

Date:

Place: Chennai

Dr.R. Maniamuthu

Post Graduate Student

Department of Prosthodontics and

Crown & Bridge,

Ragas Dental College and Hospital,

Chennai

CERTIFICATE

This is to certify that the dissertation titled “**COMPARATIVE EVALUATION OF THE WEAR RESISTANCE OF TWO DIFFERENT IMPLANT ABUTMENT MATERIALS AFTER CYCLIC LOADING – AN *IN VITRO* STUDY**” is a bonafide record work done by **Dr.R. MANIAMUTHU** under our guidance and to our satisfaction during her post graduate study period between **2016 – 2019**.

This dissertation is submitted to **THE TAMILNADU Dr. M.G.R. MEDICAL UNIVERSITY**, in partial fulfillment for the Degree of **MASTER OF DENTAL SURGERY – PROSTHODONTICS AND CROWN & BRIDGE, BRANCH I**. It has not been submitted (partial or full) for the award of any other degree or diploma.

Guided by:

Dr. Vallabh Mahadevan, M.D.S.,
Reader,
Department of Prosthodontics and
Crown & Bridge,
Ragas Dental College & Hospital,
Chennai.

Dr. N.S. Azhagarasan, M.D.S.,
Principal, Professor and Head,
Department of Prosthodontics and
Crown & Bridge,
Ragas Dental College & Hospital,
Chennai.

**THE TAMILNADU Dr. M.G.R. MEDICAL UNIVERSITY
CHENNAI**

PLAGIARISM CERTIFICATE

This is to certify the dissertation titled **“COMPARATIVE EVALUATION OF THE WEAR RESISTANCE OF TWO DIFFERENT IMPLANT ABUTMENT MATERIALS AFTER CYCLIC LOADING – AN *IN VITRO* STUDY”** of the candidate **Dr.R. MANIAMUTHU** for the award of Degree of **MASTER OF DENTAL SURGERY** in **BRANCH I - PROSTHODONTICS AND CROWN & BRIDGE.**

On verification with the urkund.com website for the purpose of plagiarism check, the uploaded thesis file contains from introduction to conclusion pages shows **4% percentage** of plagiarism, as per the report generated and it is enclosed in Annexure – VIII.

Date:

Place: Chennai

Dr.R. Maniamuthu
Post Graduate Student,
Department of Prosthodontics and
Crown & Bridge,
Ragas Dental College & Hospital,
Chennai.

Dr.Vallabh Mahadevan, M.D.S.,
Reader,
Department of Prosthodontics and
Crown & Bridge,
Ragas Dental College & Hospital,
Chennai.

**THE TAMILNADU Dr. M.G.R. MEDICAL UNIVERSITY
CHENNAI**

DECLARATION BY THE CANDIDATE

I hereby declare that this dissertation titled “**COMPARATIVE EVALUATION OF THE WEAR RESISTANCE OF TWO DIFFERENT IMPLANT ABUTMENT MATERIALS AFTER CYCLIC LOADING**” is a bonafide and genuine research work carried out by me under the guidance of **Dr.Vallabh Mahadevan, M.D.S.,** Reader, Department of Prosthodontics and Crown & Bridge, Ragas Dental College and Hospital, Chennai.

Date: 08-02-2019

Place: Chennai


Dr. Maniamuthu R

Post Graduate Student

Department of Prosthodontics and

Crown & Bridge,

Ragas Dental College and Hospital,

Chennai

CERTIFICATE

This is to certify that the dissertation titled “**COMPARATIVE EVALUATION OF THE WEAR RESISTANCE OF TWO DIFFERENT IMPLANT ABUTMENT MATERIALS AFTER CYCLIC LOADING – AN *IN VITRO* STUDY**” is a bonafide record work done by **Dr.MANIAMUTHU R** under our guidance and to our satisfaction during her post graduate study period between **2016 – 2019**.


This dissertation is submitted to **THE TAMILNADU Dr. M.G.R. MEDICAL UNIVERSITY**, in partial fulfillment for the Degree of **MASTER OF DENTAL SURGERY – PROSTHODONTICS AND CROWN & BRIDGE, BRANCH I**. It has not been submitted (partial or full) for the award of any other degree or diploma.

Guided by:



Dr. Vallabh Mahadevan, M.D.S.,
Reader,
Department of Prosthodontics and
Crown & Bridge,
Ragas Dental College & Hospital,
Chennai.

READER
DEPT. OF PROSTHODONTICS
AND CROWN & BRIDGE
Ragas Dental College & Hospital
Chennai - 600 119.



Dr. N.S. Azhagarasan, M.D.S.,
Principal, Professor and Head,
Department of Prosthodontics and
Crown & Bridge,
Ragas Dental College & Hospital,
Chennai.

Dr. N.S. AZHAGARASAN, MDS,
PRINCIPAL AND PROFESSOR & HOD,
DEPARTMENT OF PROSTHODONTICS AND CROWN & BRIDGE
RAGAS DENTAL COLLEGE AND HOSPITAL
2/102, EAST COAST ROAD, UTHANDI,
CHENNAI-600 119.

**THE TAMILNADU Dr. M.G.R. MEDICAL UNIVERSITY
CHENNAI**


PLAGIARISM CERTIFICATE


This is to certify the dissertation titled “COMPARATIVE EVALUATION OF THE WEAR RESISTANCE OF TWO DIFFERENT IMPLANT ABUTMENT MATERIALS AFTER CYCLIC LOADING – AN *IN VITRO* STUDY” of the candidate **Dr. MANIAMUTHU R** for the award of Degree of **MASTER OF DENTAL SURGERY** in **BRANCH I - PROSTHODONTICS AND CROWN & BRIDGE**.

On verification with the urkund.com website for the purpose of plagiarism check, the uploaded thesis file contains from introduction to conclusion pages shows **4% percentage** of plagiarism, as per the report generated and it is enclosed in Annexure – VIII.

Date: 08.07.2019

Place: Chennai


Dr. Maniamuthu R
Post Graduate Student,
Department of Prosthodontics and
Crown & Bridge,
Ragas Dental College & Hospital,
Chennai.


Dr. Vallabh Mahadevan, M.D.S.,
Reader,
Department of Prosthodontics and
Crown & Bridge,
Ragas Dental College & Hospital,
Chennai.

**READER
DEPT. OF PROSTHODONTICS
AND CROWN & BRIDGE
Ragas Dental College & Hospital,
Chennai - 600 119.**



RAGAS DENTAL COLLEGE & HOSPITAL

(Unit of Ragas Educational Society)

Recognized by the Dental Council of India, New Delhi

Affiliated to The Tamilnadu Dr. M.G.R. Medical University, Chennai

2/102, East Coast Road, Uthandi, Chennai - 600 119. INDIA.

Tele : (044) 24530002, 24530003-06. Principal (Dir) 24530001 Fax : (044) 24530009

TO WHOMSOEVER IT MAY CONCERN

Date: 05.02.2019

Place: Chennai

From

The Institutional Review Board,

Ragas Dental College And Hospital,

Uthandi, Chennai -600119.

The Dissertation topic titled “COMPARATIVE EVALUATION OF THE WEAR RESISTANCE OF TWO DIFFERENT IMPLANT ABUTMENT MATERIALS AFTER CYCLIC LOADING – AN *IN VITRO* STUDY” submitted by Dr. R. MANIAMUTHU, has been approved by the Institutional Review Board of Ragas Dental College and Hospital.

Dr. N. S. AZHAGARASAN, M. D. S.,

Member Secretary,

Institutional Ethics Board,

Ragas Dental College and Hospital,

Uthandi, Chennai - 600119

ACKNOWLEDGEMENT

*Its my gratitude that gives fulfillment for my study to thank experts and my well wishers who supported throughout my thesis work. I would like to express my respect and gratitude to **Professor Dr. N.S. Azhagarasan M.D.S., Principal, Professor and Head, Department of Prosthodontics & Crown and Bridge** for encouraging me to do study on this topic and his continuous support and effort for my completion by letting me to make use of amenities available in the college.*

*I would like to pay my indebted gratefulness to my Guide **Dr. Vallabh Mahadevan M.D.S., Reader, Department of Prosthodontics & Crown and Bridge** who is very supportive in bringing out best of me. I am very thankful to him to complete this study under his guidance. His calm nature helped me to clarify doubts and enriched my thesis.*

*I would like to express extremely heartfelt thanks to my **Professor Dr. JayaKrishnaKumar M.D.S.,** who gave inspiration, immense support and motivation to learn new things everyday and enlightened my thesis with his suggestions.*

*Equally my heartfelt thanks would also extends to **Professor Dr. R. Hariharan M.D.S.,** who provided good basis for my academic knowledge and encouraged to choose my thesis topic. My note of thanks will be incomplete without mentioning my greatest inspiration beloved teacher, **Professor Dr. Chitra Shankar M.D.S., Dr. R. Hariharan, M.D.S., Dr. M. Saravana Kumar, Dr. Vidhya, M.D.S., Dr. Kamatchi, M.D.S., Dr. Mahadevan, M.D.S.,** who encouraged not only in my study but also throughout my Post Graduate period to improve my knowledge.*

*I would like to thank **Dr. Ramanan, Principal, Presidency College** for his support in statistical works.*

*I would also like to thank **Mr. Ajay, Department of NanoScience and Mr. Vetrivel DST-FIST, Department of Manufacturing Technology, Anna University, Guindy** for their help in Surface profilometry and SEM work.*

*My work would not possible without the support of my family. I thank my parents **Mr.Ragupathi and Mrs. Vijayalakshmi** for their dedication and constant support. I would be grateful to my best friend and husband **Mr. R. Vishnu Prakash**, for being my backbone. Special thanks to my In-laws for their motivation towards my work.*

*I am indebted to my Seniors and Juniors **Dr.Ambedkar, Dr. Arul Kumar, Dr. Revathy, Dr. Pavan Kumar Vaddempudi, Dr. Priyadarshini, Dr. Ashwini Sukanya, Dr. Gayathree, Dr. Abinaya, Dr.SethuRaman, Dr. Aishwarya, Dr. Yasmin, Dr.Kavya, Dr. Shivasankari, Dr.Vaishali Dr. Tejaswi,**and my batchmates **Dr. Asish, Dr. Arjun, Dr.Jensy, Dr. Manimala, Dr.Samin,** my friend **Dr. Akila** for their support in my work.*

I thank God almighty who made everything good.

CONTENTS

S.NO	TITLE	PAGE NO.
1.	INTRODUCTION	1
2.	REVIEW OF LITERATURE	8
3.	MATERIALS AND METHODS	23
4.	RESULTS	41
5.	DISCUSSION	52
6.	CONCLUSION	65
7.	SUMMARY	68
8.	BIBILIOGRAPHY	71
9.	ANNEXURES	

LIST OF TABLES

TABLE NO	TITLE	PAGE NO.
1.	Basic and mean Pre-cyclic loading Surface roughness value (Pre Ra value ₁) of Group I test samples (Pre-machined Titanium straight abutments)	43
2.	Basic and mean Post-cyclic loading Surface roughness value (Post Ra value ₁) of Group I test samples (Pre-machined Titanium straight abutments)	44
3.	Basic and mean Surface roughness difference value (Ra value D ₁) of Group I test samples (Pre-machined Titanium straight abutments)	45
4.	Basic and mean Pre-cyclic loading Surface roughness value (Pre Ra value ₂) of Group II test samples (Pre-machined PEEK straight abutments)	46
5.	Basic and mean Post-cyclic loading Surface roughness value (Post Ra value ₂) of Group II test samples (Pre-machined PEEK straight abutments)	47
6.	Basic and mean Surface roughness difference value (Ra value D ₂) of Group II test samples (Pre-machined PEEK straight abutments)	48
7.	Comparative evaluation of the mean pre-cyclic loading and post cyclic loading surface roughness values for Group I test samples (Pre-machined Titanium straight abutments)	49
8.	Comparative evaluation of the mean pre-cyclic loading and post cyclic loading surface roughness values for Group II test samples (Pre-machined PEEK straight abutments)	50

9.	Comparative evaluation of the mean difference values of pre and post-cyclic loading Surface roughness (Ra value) of Group I (Pre-machined Titanium straight abutments) and Group II test samples (Pre-machined PEEK straight abutments)	51
----	---	-----------

ANNEXURE I

METHODOLOGY- OVERVIEW

ANNEXURE II

CALIBRATION CERTIFICATE FOR CYCLIC LOADING MACHINE

ANNEXURE III

LIST OF FIGURES

Fig.No.	Title
Fig.1	: Titanium dental implant standard platform 4.2mm diameter, 10 mm length (NORIS)
Fig.1 a	: Vial containing implant
Fig.1b	: NORIS dental implant
Fig.2	: Premachined titanium abutment, standard platform, internal hexagon
Fig.2 a	: Manufacturer packaging
Fig.2b	: Abutment
Fig.3	: Pre machined PEEK abutment, standard platform, internal hexagon
Fig. 3a	: Manufacturer packaging
Fig.3b	: Abutment
Fig.4	: Hex driver
Fig.5	: Torque wrench
Fig.6	: Clear autopolymerising acrylic resin (monomer and polymer)
Fig.7	: Type I Glass Ionomer luting cement
Fig.7a	: Mixing pad

Fig.7b	: Agate spatula
Fig.7c	: Plastic instrument
Fig.8	: Die lubricant
Fig.9	: Spirit level indicators
Fig.10	: Burs
Fig.11	: Inlay wax
Fig.12	: PKT instruments
Fig.13a	: Sprue wax
Fig.13b	: Silicone investment ring
Fig. 13c	: Crucible former
Fig.13e	: Surfactant spray
Fig.13d	: Phosphate bonded investment material for Ni-Cr alloy
Fig.13f	: Colloidal silica
Fig.14	: Ni-Cr Pellets
Fig.15	: Crucible Former
Fig.16	: Stainless Steel Block
Fig.17	: Dental surveyor
Fig.18	: Vacuum mixer
Fig.19	: Burnout furnace
Fig.20	: Induction casting machine
Fig.21	: Custom made Cyclic Loading machine
Fig.22	: Custom made positioning jig
Fig.23	: Surface Profilometer (Talysurf CCI Lite)

- Fig.24** : Scanning Electron Microscope S-3700N(Hitachi High Technologies Corporation, Japan)
- Fig.25** : Fabrication of stainless steel block
- Fig.25a** : Stainless steel block
- Fig.25b** : Line diagram of stainless steel block
- Fig.26** : Connecting implant and abutments.(Group I)
- Fig.26a** : Titanium Abutment
- Fig.26b** : Titanium Implant
- Fig.27** : Paralleling the surveying platform with the spirit level indicators
- Fig.28** : Placing titanium implant abutment assembly in the stainless steel block
- Fig.29** : Placement of acrylic resin around the implant abutment assembly (titanium abutment)
- Fig.30** : Mounted resin block with the reference marks for orientation (titanium abutment)
- Fig.31** : Connecting implant and abutments.(Group II)
- Fig.31a** : PEEK Abutment
- Fig.31b** : Titanium Implant
- Fig.32** : Placing titanium implant and PEEK abutment assembly in the stainless steel block
- Fig.33** : Placement of acrylic resin around the implant abutment assembly (PEEK abutment)
- Fig.34** : Mounted resin block with the reference marks for orientation (PEEK abutment)
- Fig.35** : Group I Test samples

Fig.36 : Group II Test samples

Fig.37A : Surface Profilometry done for analysis of surface roughness before loading

Fig.37Aa : Titanium abutment

Fig.37Ab : PEEK abutment

Fig.37B : Scanning Electron Microscopy before loading

Fig.37Ba : Microscope

Fig.37Bb : Samples

Fig.38 : Fabrication of cement retained Ni-Cr cast crowns

Fig.38a : Wax pattern preparation

Fig.38b : Spruing and investing

Fig.38c : Burnout and casting

Fig.38d : Trimming and finishing the crowns

Fig.38d : Trimming and finishing the crowns

Fig.38e : Finished crowns

Fig.39 : Group I Test samples with crowns

Fig.40 : Group II Test samples with crowns

Fig.41 : Cyclic loading

Fig.42A : Surface Profilometry done for analysis of surface roughness after loading

Fig.42Aa : Titanium abutment

Fig.42Ab : PEEK abutment

Fig.42B : Scanning Electron Microscopy after loading

Fig.42Ba : Microscope

Fig.42Bb : Samples

ANNEXURE-IV

GRAPHS

GRAPH NO	TITLE
1.	Basic Pre-cyclic loading Surface roughness values (Pre Ra value ₁) of Group I test samples (Pre-machined Titanium straight abutments)
2.	Basic Post-cyclic loading Surface roughness values (Post Ra value ₁) of Group I test samples (Pre-machined Titanium straight abutments)
3.	Basic Pre and Post loading Surface roughness (Ra value D ₁) differences of Group I test samples (Titanium pre-machined straight abutments)
4.	Basic Pre-cyclic loading Surface roughness values (Pre Ra value ₂) of Group II test samples (Pre-machined PEEK straight abutments)
5.	Basic Post-cyclic loading Surface roughness values (Post Ra value ₂) of Group II test samples (Pre-machined PEEK straight abutments)
6.	Basic pre and post-cyclic loading Surface roughness difference values (Ra value D ₂) of Group II test samples (PEEK pre-machined straight abutments)

7. Comparative evaluation of the mean pre-cyclic loading and post cyclic loading surface roughness (Ra Value) values of Group I test samples (Pre-machined Titanium straight abutments)
8. Comparative evaluation of the mean pre-cyclic loading and post cyclic loading surface roughness (Ra Value) values of Group II test samples (Pre-machined PEEK straight abutments)
9. Comparative evaluation of the mean pre and post- cyclic loading Surface roughness (Ra value) of Group I (Pre-machined Titanium straight abutments) and Group II test samples (Pre-machined PEEK straight abutments)

ANNEXURE – V

ADVANCED 3D SURFACE TEXTURE PHOTOMICROGRAPHY OF THE SURFACE ROUGHNESS OF GROUP I AND GROUP II TEST SAMPLES BEFORE AND AFTER CYCLIC LOADING

Fig.No.	TITLE
Fig. 40:	Advanced 3D view of surface topography of Group I (Titanium Abutment) before cyclic loading
Fig. 41:	Advanced 3D view of surface topography of Group I (Titanium Abutment) after cyclic loading
Fig. 42:	Advanced 3D view of surface topography of Group II (PEEK Abutment)before cyclic loading
Fig. 43:	Advanced 3D view of surface topography of Group II (PEEK Abutment) after cyclic loading

ANNEXURE – VI

**SCANNING ELECTRON MICROSCOPE
PHOTOMICROGRAPHY FROM GROUP I AND GROUP II
REPRESENTATIVE TEST SAMPLE BEFORE AND AFTER
CYCLIC LOADING**

Fig.No.	TITLE
Fig. 43:	SEM micrographs at magnifications 500X and 1000X shows surface with presence of voids and irregularities before cyclic loading of Group I test samples
Fig. 44:	SEM micrographs at magnifications 500X and 1000X shows surface with diminished voids and reduction in irregularities representing wear after cyclic loading of Group I test samples
Fig. 45:	SEM micrographs at magnifications 500X and 1000X shows surface with less irregularities before cyclic loading of Group II test samples respectively
Fig. 46:	SEM micrographs at magnifications 500X and 1000X shows surface with increased irregularities after cyclic loading of Group II test samples

ANNEXURE – VII

ENERGY DISPERSIVE X-RAY SPECTROPHOTOMETRY FROM GROUP I AND GROUP II REPRESENTATIVE TEST SAMPLE BEFORE AND AFTER CYCLIC LOADING

S.No.	TITLE
1.	Energy Dispersive X-Ray Spectrophotometry before cyclic loading of Group I test samples
2.	Energy Dispersive X-Ray Spectrophotometry after cyclic loading of Group I test samples
3.	Energy Dispersive X-Ray Spectrophotometry before cyclic loading of Group II test samples
4.	Energy Dispersive X-Ray Spectrophotometry before cyclic loading of Group II test samples

INTRODUCTION

Rehabilitation of partially and completely edentulous arches utilizing dental implants have become a well established treatment modality with an overall success rate of 89.7% over 15 years.^{1,29} Clinical expertise, techniques and continued research and development of implant biomaterials have significantly introduced newer avenues in oral implantology.^{25,31}

The predictable nature of osseointegration has provided innovative treatment techniques overcoming challenges associated in implant based restoration. However, standard protocol of two stage implant system results in microgap at implant abutment interface and act as a reservoir for microbial colonization.^{4,11,37}

The introduction of individually designed abutments by means of computer-aided design and manufacturing (CAD/CAM), have revolutionized the customization of abutments to suit the individual functional and esthetic demands.^{19,20} Besides its esthetic requirements, implant abutment has gained more importance with respect to peri implant health due to its increased contact with the peri implant tissues especially when cement retained restorations are used.^{20,21,35}

Implant abutment connection mainly depends on the type of connection and mating potential.^{4,37,52} The commonly used abutments in different implant systems are external hexagon, internal hexagon, cylinder hex, conical, octagonal, spline cam, cam tube, pin/slot. The external hexagon was the oldest connection that was mainly indicated for completely edentulous arch restorations, however, when used for partially edentulous arches it had some shortcomings like screw loosening and compromised screw joint stability.^{4,7,38.}

In order to overcome these mechanical problems, internal hexagon has gained importance due to its design characteristics such as reduced vertical height platform for restorative components, distribution of stresses within the long axis of the implant thus resisting joint opening which is suitable for one-stage implant installation and single tooth restoration where there is off-axis loading.^{4,8,37,52}

This type of connection along with the abutment bio-material directly influences the stability of abutments during aging.⁴⁹ So, the biomaterials from which the implant abutments are fabricated, needs a thorough evaluation as there is differential wear rates between the implant platform and abutment during physiological loading which may result in the formation of microgap.^{7,23,55}

Traditionally, implant abutments are manufactured from the titanium due to its very high resistance to corrosion and good biocompatibility.^{14,19,40} However, due to the metallic nature of titanium, esthetics of the implant restoration is

compromised resulting in graying of the peri implant tissues mainly when the soft tissue thickness is less than 2 mm.^{8,14,32,47}

The need for improved esthetics led to the development of metal free abutments, so materials such as ceramics and polymers were used for the manufacturing of implant abutments. Sintered alumina were used which shows less fracture resistance.^{19,24,28,35} Then the zirconia abutments were introduced which has good biocompatibility. The esthetics is also enhanced as it has high flexural strength but there was a decrease in toughness and strength and sensitive to temperature changes. Since zirconia abutments are more opaque, the shade difference have to be matched by addition of more porcelain.^{15,37,40,47,50,56,58}

The various factors affecting the stress or energy transfer between the implant and peripheral bone are the direction of loading, the design and material characteristics of implant and/or implant crown.^{19,20} A common problem occurred in implant supported restorations with either metal or zirconia core was chipping of porcelain due to stress concentration on the restoration. As the implant bone interface shows less resilience or no micro-movement due to decrease in proprioception, the load concentration on the restoration causes bone resorption and subsequent implant failure.¹⁹

The chipping and fracture of restorative material which was used in the past was reduced by the introduction of newer resin based restorative materials and CAD-CAM technology. Recently, synthetic tooth coloured polymeric

thermoplastic material named PEEK has gained popularity as a dental restorative material.¹⁹

PolyEtherEtherKetone (PEEK), belonging to the family of PolyArylEtherKetone(PAEK) has good mechanical properties, chemical inertness and biocompatibility. The most beneficial property of PEEK is its elastic modulus which is equivalent to elastic modulus of human bone. Considering these properties, implants and its abutments are fabricated using PEEK.^{24,31}

There are studies comparing the properties of PEEK and titanium abutments in which Koutouzis et al²⁴ suggested that there is no significant difference in the bone resorption and soft tissue inflammation around the PEEK and titanium abutments. Furthermore, the biofilm formation on PEEK abutments was comparable to those made of titanium, zirconia and polymethylmethacrylate.²⁴

Stress shielding is the reduction in volume of the bone around an implant due to the shielding of normal loads by the implant. Since, PEEK has elastic modulus equivalent to that of human bone, the stress shielding effect is reduced and the bone resorption around the PEEK implant and its abutment is nullified.^{10,29,33,37,40,41,44}

The most important physical property of a restorative material is its wear resistance. The various factors influencing the wear of the material are its contact, surface roughness, velocity, load, temperature and lubrication.^{23,47,48}

Most of the abutments, fail at the area of connection.^{14,38} When abutment with internal conical connection are used and the force is applied at the angle of 30° to implant axis, representing the maxillary anterior region, the output load applied in this area of the internal cone of the abutment.¹⁴ Thus, stress concentration and torque are higher in the internal cone of the abutment, which explains the failure of abutment at the area of connection.¹⁴

In the anterior region bite forces were found to be 140 N. The physiological maximum incisor biting forces may be upto 290 N depending on facial morphology and age.^{13,18} The simulation of mastication is a preclinical method of studying the materials and devices which create forces comparable to those which develop during horizontal and vertical components of masticatory motion. Cyclic loading test have been employed to simulate the clinical loading conditions. The irregularities generated during manufacturing may be minimized by mechanical cycling.^{23,46,57}

In the study performed by Stimmelmayer et al⁴⁷, the wear of the interface of titanium implants connected with one piece zirconia and titanium abutments were measured.⁴⁷ SEM micrographs were used to analyse the wear before and after cyclic loading, only minimal wear or abrasion was noticeable on the titanium abutment than one piece zirconia abutment.⁴⁷ The metal erodes and wears when

the ceramic and metal meets. SEM analysis alone cannot confirm this, because it might have occurred during the test due to the amount of debris created.^{23,47}

In the present study Scanning Electron Microscope and Energy Dispersive X-Ray Spectrophotometry method is used for the wear analysis. The Scanning Electron microscope (SEM) which is closely related to electron probe, is designed primarily for producing electron images, but can also be used for element mapping and even point analysis, if an X-Ray spectrophotometer is added. So, EDS makes use of the X-ray spectrum emitted by a solid sample bombarded with a focused beam of electrons to obtain a localized chemical analysis.^{23,47}

Surface profilometry is also used in this study as an additional tool for quantitative assessment of surface roughness (Ra value) of abutments which were dynamically loaded. Surface roughness correlates with the wear behavior of the abutment material.⁴⁷

In the light of the above, the aim of this present study is comparative evaluation of the wear resistance of two different abutment materials with the effect of cyclic loading.

The null hypothesis is as the elastic modulus of PEEK is lower than the Titanium, the wear of the PEEK abutment will be expected to be higher when compared to the Titanium abutment.

The objectives of the present study included the following:

- To measure the wear values of Titanium premachined abutments before cyclic loading (GROUP I).
- To measure the wear values of PEEK premachined abutments before cyclic loading (GROUP II).
- To measure the wear values of Titanium premachined abutments after cyclic loading (GROUP I).
- To measure the wear values of PEEK premachined abutments after cyclic loading (GROUP II).
- To compare the wear values of Titanium premachined abutments before and after cyclic loading (GROUP I).
- To compare the wear values of PEEK premachined abutments before and after cyclic loading (GROUP II).
- To compare the wear values of both Titanium and PEEK premachined abutments before and after cyclic loading (GROUP I Vs GROUP II).

REVIEW OF LITERATURE

Scheller et al(1998)⁴² demonstrated that stable long-term results can be achieved when replacing single teeth with Brånemark implants and cemented crowns on CeraOne abutments. The overall cumulative success rate was 95.9% for implants and 91.1% for crowns. Mean marginal bone resorption was well within the limits set by Albrektsson et al in 1986. Bone resorption around these restorations was minimal following the first-year remodeling phase, and the status of soft tissues remained stable. Changing the abutment screw from titanium to gold seemed to resolve the problem with loosening of abutment screws.

Sawase T et al (2000)⁴¹ investigated the surface characteristics of 5 commercially available implant abutments which were Brånemark (Nobel Biocare, Gothenburg, Sweden), Astra (AstraTech, Mölndal, Sweden), IMZ (Friatec, Mannheim, Germany), STERIOSS (Denar, CA, USA) and POI (Kyocera, Kyoto, Japan). The three dimensional imaging and analysis of the surface topography were carried out using a confocal laser scanning

profilometer (TopScan 3D). The chemical composition of abutment surfaces was analyzed by Auger Electron Spectroscopy (AES). The specimens which were investigated in this study varied in their topography and elemental composition. These variations were strongly due to the manufacturing processes which were milling, polishing, cleaning and sometimes oxidation methods.

De Avila et al(2007)¹⁵ evaluated the effect of 2 commercially available implant abutment materials on the adhesion phase and biofilm formation. Ti presented lower hydrophobicity and surface free energy values than the ZrO₂, and 6.1-fold fewer bacteria adhered to the Ti. After 48 hours, detailed quantitative analysis showed that biofilm biomass and biofilm density were lower on the Ti disks than on ZrO₂. The quantity of phylotypes on the Ti and ZrO₂ surfaces was relatively similar during the attachment and early biofilm formation periods. Although no difference in the bacteria profile was observed between both materials independent of the time point, the highest level of colonization was on ZrO₂.

Tetelman et al(2008)⁴⁸ presents 3 cases that demonstrate a team-centered approach in using a poly (acrylether) ketone plastic provisional abutment (Peek). This abutment, cost-effective and easily modified, supports a transitional prosthesis that is delivered at the time of implant placement.

Yuzugullu B et al(2008)⁵⁶ assessed the implant-abutment interface after the dynamic loading of titanium, alumina, and zirconia abutments. A mechanical testing machine applied compressive dynamic loading between 20 and 200 N at 1 Hz on a standard contact area of copings cemented on abutments for 47.250 cycles. The measurements of microgaps at the implant-abutment interface from the labial, palatinal, mesial, and distal surfaces of each specimen were undertaken by scanning electron microscope analyses prior to and after the experiments. Owing to their comparable microgap values at the implant-abutment interface after the dynamic loading, ceramic abutments can withstand functional forces like conventional titanium abutments

Ribeiro CG et al(2009)³⁷ compared three implant-abutment interfaces (external hexagon, internal hexagon and cone-in-cone) regarding the fatigue resistance of the prosthetic screw. Although internal connections present a more favorable design, this study did not show any advantage in terms of strength. The external hexagon connector used in this study yielded similar results to those obtained in a previous study with Nobel Biocare and Straumann systems. However, the internal connections (cone-in-cone and internal hexagon) were mechanically inferior compared to previous results.

Sailer et al(2009)³⁹ systematically reviewed the 5-year survival rates and incidences of complications associated with ceramic abutments and to compare them with those of metal abutments. Esthetic complications tended to be more frequent at metal abutments. A meta-analysis of the laboratory data was impossible due to the non-standardized test methods of the studies included. The 5-year survival rates estimated from annual failure rates appeared to be similar for ceramic and metal abutments. The information included in this review did not provide evidence for differences of the technical and biological outcomes of ceramic and metal abutments.

Santing HJ et al(2010)⁴⁰ evaluated the fracture strength of implant-supported composite resin crowns on PEEK and solid titanium temporary abutments, and to analyze the failure types. The failure types were analyzed and further categorized as irreparable (Type 1) or reparable (Type 2). No significant difference was found between different abutment types. The most frequently experienced failure types were cohesive fractures of the composite resin crowns (75 out of 104), followed by screw loosening (18 out of 104). According to reparability, the majority of the specimens were classified as Type 1 (82 out of 104). Type 2 failures were not often observed (22 out of 104). Provisional crowns on PEEK abutments showed similar fracture strength as titanium temporary abutments except for central incisors. Maxillary right central incisor composite resin crowns on PEEK temporary abutments fractured below the mean anterior masticatory loading forces reported to be approximately 206 N.

Klotz et al (2011)²³ used a clinical simulation to determine whether wear of the internal surface of a titanium implant was greater following connection and loading of a one-piece zirconia implant abutment or a titanium

implant abutment. The method was able to quantify the area of material transferred to the abutments. There was considerably more wear associated with the zirconia abutments, but the rate of wear slowed after about 250,000 cycles. The implants with the zirconia abutments showed a greater initial rate of wear and more total wear than the implants with the titanium abutments following cyclic loading. The amount of titanium transfer seen on the zirconia abutment increased with the number of loading cycles but appeared to be self-limiting. The clinical ramifications of this finding are unknown at this time; however, the potential for component loosening and subsequent fracture and/or the release of particulate titanium debris may be of concern.

Koutouzis et al(2011)²⁴ comparatively evaluated soft and hard tissue responses to titanium and polymer provisional implant abutments over a 3-month period and concluded implants temporally restored with PEEK or titanium healing abutments indicate that PEEK healing abutments do not render an increased risk for marginal bone loss and soft tissue recession during the initial healing period.

Saidin S et al (2012)³⁸ analysed micromotion and stress distribution at the connections of implants and four types of abutments: internal hexagonal, internal octagonal, internal conical and trilobe. The internal hexagonal and octagonal abutments produced similar patterns of micromotion and stress distribution due to their regular polygonal design. The internal conical abutment produced the highest magnitude of micromotion, whereas the trilobe connection showed the lowest magnitude of micromotion due to its polygonal profile. Non-cylindrical abutments provided a stable locking mechanism that reduced micromotion, and therefore reduced the occurrence of microgaps. However, stress tends to concentrate at the vertices of abutments, which could lead to microfractures and subsequent microgap formation.

Stimmelmayer M et al(2012)⁴⁴ measured the wear of the interface between titanium implants and one-piece zirconia abutments in comparison to titanium abutments. Abutment fracture or screw loosening was not observed during cyclical loading. Comparing the microscope and SEM images more wear was observed on the implants connected to zirconia abutments. Titanium implants showed higher wear at the implant interface following cyclic loading

when connected to one-piece zirconia implant abutments compared to titanium abutments. The clinical relevance is not clear; hence damage of the internal implant connection could result in prosthetic failures up to the need of implant removal.

Wang et al (2013)⁵³ compared maximum deformation and failure forces at the implant–abutment interface of titanium implants between titanium-alloy and zirconia abutments with two levels of marginal bone loss and concluded that the maximum deformation and failure forces are lower for implants with a marginal bone loss of 3.0 mm than of 1.5 mm. Zirconia abutments can withstand physiological occlusal forces applied in the anterior region.

Neumann et al(2014)³² compared the fracture resistance of abutment retention screws made of titanium, polyetheretherketone (PEEK) and 30% carbon ber-reinforced PEEK, using an external hexagonal implant/UCLA-type abutment interface assembly. In a universal testing machine, 45° off-axis and 200 N load (static load) was applied at the central point of the abutment

extremity, at a crosshead speed of 5 mm/minute, until failure. Finally, visual analysis of the fractions revealed that 100% of them occurred at the neck of the abutment screw, suggesting that this is the weakest point of this unit. PEEK abutment screws have lower fracture resistance, in comparison with titanium abutment screws.

Najeeb et al(2016)³¹ reviewed to summarize the outcome of research conducted on the material for dental applications. In addition, future prospects of PEEK in the field of clinical dentistry have been highlighted. PEEK has been explored for a number of applications for clinical dentistry. For example, PEEK dental implants have exhibited lesser stress shielding compared to titanium dental implants due to closer match of mechanical properties of PEEK and bone. PEEK is a promising material for a number of removable and fixed prosthesis. Furthermore, recent studies have focused improving the bioactivity of PEEK implants at the nanoscale. Considering mechanical and physical properties similar to bone, PEEK can be used in many areas of dentistry. Improving the bioactivity of PEEK dental implants without compromising their mechanical properties is a major challenge. Further

modifications and improving the material properties may increase its applications in clinical dentistry.

Rea et al(2016)³⁵ evaluated the marginal soft and hard tissue healing at titanium and Polyetheretherketone (PEEK) healing implant abutments over a 4-month period. A higher resorption of the buccal bone crest was observed at the PEEK bonded to a base made of titanium abutments (1.0 0.3 mm) compared to those made of titanium (0.3 0.4 mm). However, similar dimensions of the peri-implant mucosa and similar locations of the soft tissues in relation to the implant shoulder were observed. No statistically significant differences were seen in the outcomes when the pristine PEEK was compared with the roughened PEEK abutments. The mean apical extension of the junctional epithelium did not exceed the implant shoulder at any of the abutment types used. The coronal level of the hard and soft tissues allows the conclusion that the use of PEEK as healing abutments may be indicated.

Val et al(2016)⁵¹ assessed the effectiveness of using non-titanium abutments for better establishment of peri-implant biological width and to

assess the stability of the soft tissue. Histological, histomorphometric, ISQ and radiological analyses were performed. After an 8- week postoperative period, all implants showed an appropriate primary stability for loading protocols, and no statistical difference was found between the groups. Reinforced PEEK constitute an effective alternative to conventional titanium abutments, given its high rate of biocompatibility, preservation of bone height and soft tissue stability.

Hahnel et al(2017)¹⁹ investigated the formation of biofilms on the surface of materials applied for the fabrication of implant abutments. Within the limitations of a laboratory study, the results suggest that biofilm formation on the surface of PEEK is equal or lower than on the surface of conventionally applied abutment materials such as zirconia and titanium. However, clinical studies are necessary to corroborate these preliminary results.

Kaleili et al (2017)²⁰ evaluated the biomechanical behaviors of resin-matrix ceramics and PEEK customized abutments in terms of stress distribution in implants and peripheral bone. Six different models were created according to combinations of restoration materials (translucent zirconia [TZI], lithium disilicate glass ceramic [IPS], polymer-infiltrated hybrid ceramic

[VTE]), and customized abutment materials (PEEK and zirconia). In each model, the implants were loaded vertically (200 N) and obliquely (100 N). The stress distribution in the crown, implant and abutments was evaluated through the von Mises stress analysis, and the stress distribution in the peripheral bone was examined through the maximum and minimum principal stress analyses.

Schwitilla et al(2017)⁴³ determined the average insertion torque (IT) at failure of this design, so as to determine its suitability for immediate loading, which requires a minimum IT of 32 N·cm. The average IT values at failure of the unfilled PEEK implants were measured at 22.6 ± 0.5 N·cm and were significantly higher than those of the CFR-Implants (20.2 ± 2.5 N·cm). The average IT values at failure of the titanium specimens were significantly higher (92.6 ± 2.3 N·cm) than those of the two PEEK variants. PEEK- and CFR-PEEK-implants in the present form cannot adequately withstand the insertion force needed to achieve primary stability for immediate loading. Nevertheless, the achievable torque resilience of the two PEEK-variants may be sufficient for a two-stage implantation procedure. To improve the torque resistance of the PEEK implant material the development of a new manufacturing procedure is necessary which reinforces the PEEK base with continuous multi-directional carbon fibers as opposed to the axially parallel fibers of the tested PEEK compound.

Watkin A et al(2017)⁵⁴ tested five types of implant restorations using titanium, zirconia and lithium disilicate abutments after being subjected to

long-term fatigue loading. Groups Ti, ZrT, LaT and LcT withstood 1,200,000 fatigue load cycles and higher forces than physiological occlusal forces without fracture or debonding of the ceramic suprastructure. In group Zr, some specimen did not survive the chewing simulation and this group showed the lowest resistance to failure with a median of 198 N. Within the limitations of this study, it could be concluded that lithium disilicate abutments and hybrid-abutment-crowns show promising durability and strength after long-term dynamic loading. The use of titanium base enhances the strength of the zirconia abutments.

de Carvalho *et al* (2018)¹⁰ evaluated the compressive strength (CS) of protocol bars on polyether ether ketone (PEEK) implants compared to metallic bars (NiCr). Compression strength (N) and counter torque (N/cm) data were analyzed with two criteria: ANOVA and Tukey ($\alpha = 0.05$). PEEK bars showed lower compression strength than that verified for metallic bars.

ElHoussiney AG *et al* (2018)¹³ compared the failure events and incidence of complications of different abutment materials in anterior and posterior regions. Failure was defined as complete loss of the abutment requiring replacement by a new abutment. A total of 863 and 1,264 implants

were inserted in the anterior and posterior regions, respectively, in a total of 1,529 patients. No titanium abutments failed in anterior or posterior regions. On the other hand, 1.6% of zirconia abutments failed in the anterior region and 1.5% failed in the posterior region. Technical complications occurred mostly in the posterior region and mostly involved zirconia abutment. Meta-analysis was possible only for zirconia-abutment failure, due to considerable heterogeneity of studies and outcome variables. No significant difference in failure rate was found between anterior and posterior zirconia abutments (risk ratio 1.53, 95% CI 0.49–4.77; $P=0.47$). This systematic review and meta-analysis showed similar outcomes of different abutment materials when used in anterior and posterior regions in terms of failure events and biological and aesthetic complications. The only significant finding was the increased incidence of technical complications in the posterior region, mostly involving zirconia abutments. Abutment-screw loosening was the most common technical complication.

MATERIALS AND METHODS

The present *in vitro* study was conducted to comparatively evaluate the wear resistance of two different implant abutment materials after cyclic loading.

The following materials and equipments were used for the study:

MATERIALS EMPLOYED

- Titanium dental implant, standard platform, internal hexagon, 4.2 mm diameter, 10 mm length (NORIS Dental Implants) **(Fig: 1:a,b)**
- Premachined titanium abutment, standard platform, internal hexagon (NORIS Dental Implants). **(Fig: 2:a,b)**
- Premachined PEEK abutment, standard platform, internal hexagon (NORIS Dental Implants). **(Fig: 3:a,b)**
- Clear autopolymerizing acrylic resin (RR Cold Cure., DPI, India) **(Fig: 6)**
- Sprue wax (Ref 40085, Bego, Germany) **(Fig: 13)**
- Silicone investment ring (Sili Ring., Delta labs, Chennai, India) **(Fig: 13)**
- Crucible former (Sili Ring., Delta labs, Chennai, India) **(Fig: 15)**
- Surfactant spray (Aurofilm., Bego, Germany) **(Fig: 13)**
- Colloidal silica (Begosol., Bego, Germany) **(Fig: 13)**

- Phosphate bonded investment material for Cobalt Chromium alloy(Wirovest., Bego, Germany) **(Fig: 13)**
- Die lubricant (Yeti Dental, Germany) **(Fig: 8)**
- Inlay casting wax (GC Corporation, Tokyo, Japan) **(Fig: 11)**
- Phosphate bonded investment material for Nickel Chromium alloy(Bellasun., Bego, Germany) **(Fig: 13)**
- Nickel Chromium (Ni-Cr) alloy pellets (Bellabond plus., Bego, Germany) **(Fig: 14)**
- Type I glass ionomer luting cement (powder and liquid) (GC Corporation.,Tokyo, Japan) **(Fig:7)**

INSTRUMENTS USED:

- Hex driver (NORIS Dental Implants., Israel) **(Fig: 4)**
- Long calibrated torque wrench (NORIS Dental Implants., Israel) **(Fig: 5)**
- Spirit level indicators (JinhuaHengda tools, China) **(Fig: 9)**
- PKT instruments (Delta Labs, Chennai, India) **(Fig: 12)**
- Carborundum separating discs and mandrel (Dentorium., New York, U.S.A) **(Fig: 10)**
- Tungsten carbide metal trimming burs (Edenta., Switzerland) **(Fig: 10)**
- Mixing pad (GC Corporation., Tokyo, Japan) **(Fig: 7)**
- Plastic spatula (GC Corporation., Tokyo, Japan) **(Fig: 7)**

EQUIPMENTS USED:

- Dental surveyor (Saeshin Precision Ind. Co., Korea) **(Fig: 17)**
- Vacuum mixer (Whipmix, Kentucky, U.S.A.) **(Fig: 18)**
- Surface profilometer (Talysurf CCI Lite) **(Fig: 23)**
- Scanning Electron Microscope S-3700N (Hitachi High Technologies Corporation, Japan) **(Fig: 24)**
- Burnout furnace (Technico laboratory products Pvt. Ltd., Chennai, India) **(Fig: 19)**
- Induction casting machine (Fornax, Bego, Germany) **(Fig: 20)**
- Custom-made cyclic loading machine (Designed & Manufactured by Lokesh Industries, Chennai) **(Fig: 21)**
- Custom-made positioning Jig (Designed & Manufactured by Lokesh Industries, Chennai) **(Fig: 22)**

Description of the custom-made cyclic loading machine: (Fig.21)

In the present study, to simulate the test samples in function, a custom made cyclic loading machine was used that aids in analysis of wear with the effect of cyclic loading. The machine has a motor with a gear box; the motor rotates and compresses a spring, which on elongation applies a loading force on the test sample. The calibration of this equipment is described below:

Specification of motor:

90 watts, Single phase 230V, Continuous rating, motor giving 1350 RPM with gear reduction box of 1:18 giving a final RPM of 75 (Swipe Industries, Pune, India).

Specification of spring:

Spring load spring ISO 10243:2010 (Special Springs, Rosa, Italy)

Hole diameter – 16 mm, Rod diameter – 8 mm

Free Length of spring – 38 mm

Spring constant – 48.5 N/mm

Specification of timer:

999 minutes timer with time memory (K-Pas, Chennai, India)

The motor was connected to an eccentric cam of 2.5 mm, which rotated when the motor was turned on. The 2.5 mm eccentric cam compressed a spring to the same length as it rotated generating a load of approximately 250N. The spring transmitted the load to the stylus (3 mm diameter), which transmitted a lesser load of approximately 200 N to the sample due to energy loss.

Calibration of custom-made cyclic loading device:

The maximum and minimum loads delivered by the custom-made cyclic loading device were calibrated by a professional load calibration agency (Hi Tech Calibration Services, Chennai, India).

Calibrated Results:

Auto mode : Max. Load: 230.2 N, Min. Load: 0.2N

Manual mode : Max. Load: 225.9 N, Min. Load: 0.2N

Description of Custom-made positioning Jig:

The custom-made positioning jig was used to orient the sample for loading in the cyclic loading machine. The custom-made jig consists of a platform and bolt. The sample when placed in the jig platform is automatically positioned at 30° angulation to the platform and can be secured in place with the help of a bolt.

Description of Scanning electron microscope (Fig: 23)

Scanning electron microscope (SEM) is a type of electron microscope that produces images of a sample by scanning the surface with a focused beam of electrons. The electrons interact with atoms in the sample, producing various signals that contain information about the surface topography and composition of the sample. The electron beam is scanned in a raster scan pattern, and the position of the beam is combined with the detected signal to produce an image. SEM can achieve resolution better than 1 nanometer. Specimens are observed in high vacuum in conventional SEM, or in low vacuum or wet conditions in variable pressure or environmental SEM, and at a wide range of cryogenic or elevated temperatures with specialized instruments are the good options in material analysis offering the leading imaging solution. With a motorised 5 axis stage with large XY and Z travels, variable pressure capability as standard and easy to use PC-SEM software, and it offers a perfect imaging solution. It has a working distance of 10 mm and a magnification of 5x- 3,00,000x. The most common SEM mode is the detection of secondary electrons emitted by atoms

excited by the electron beam. The number of secondary electrons that can be detected depends, among other things, on specimen topography. By scanning the sample and collecting the secondary electrons that are emitted using a special detector, an image displaying the topography of the surface is created.

For conventional imaging in the SEM, specimens must be electrically conductive, at least at the surface and electrically grounded to prevent the accumulation of electrostatic charge. Metal objects require little special preparation for SEM except for cleaning and conductively mounting to a specimen stub. Non-conducting materials are usually coated with an ultrathin coating of electrically conducting material, deposited on the sample either by low-vacuum sputter coating or by high-vacuum evaporation. Conductive materials in current use for specimen coating include gold, gold/palladium alloy, platinum, iridium, tungsten, chromium, osmium, and graphite.

Non- contact 3D Profilometer (Fig: 22)

3D Profilometer instrument (Taylor Habson, Pennsylvania) works on the principal of using LASER beam as a sensor to detect the surface roughness of the abutment at the implant abutment interface. The surface of the abutment at the implant abutment interface with reference to a particular mid labial point were analyzed before after cyclic loading with this equipment The 3D-Non contact Profilometer is designed with loading edge chromatic confocal optical technology (Axial chromatism). A classical instrument is the profilograph from an English company Taylor Hobson with an electromagnetic sensor.

After amplification of the electric signal, there is a graphic record of the curve at the output of the profilograph, which is corresponding to the surface micro-roughness on defined length of the sample, alternatively a corresponding sequence of values which can be now stored in digital memory and other evaluations be done by using common software. It can measure any material without any image stitching; this type of profilometer can generate 3D- images as well as average surface mean roughness (Ra) values.

The measurements of the height and depth of the roughness profile before and after cyclic loading can be compared.

METHODOLOGY

1. Fabrication of stainless steel block.
2. Preparation of Group I test samples (Titanium abutment)
 - i) Attachment of Titanium abutments to implants.
 - ii) Placement of implant abutment assembly in the stainless steel block.
 - iii) Embedding procedure of implant abutment assembly with acrylic resin.
3. Preparation of Group II test samples (PEEK abutment)
 - i) Attachment of PEEK abutments to implants.
 - ii) Placement of implant abutment assembly in the stainless steel block.
 - iii) Embedding procedure of implant abutment assembly with acrylic resin.
4. Grouping of test samples
5. Quantitative and qualitative analysis of test samples before cyclic loading
 - i. Surface profilometry.
 - ii. SEM.
6. Fabrication of cement retained Ni-Cr cast crowns
 - i. Preparation of wax pattern.
 - ii. Spruing, Investing and Burn out of wax pattern.
 - iii. Casting Divesting and finishing the crown.
7. Cementation of cement retained Ni-Cr cast crowns

8. Cyclic loading of test samples
9. Decementation of crown
10. Quantitative and qualitative analysis of test samples after cyclic loading
 - i. Surface profilometry.
 - ii. SEM.
11. Data tabulation and Statistical analysis

1. Fabrication of stainless steel block: (Fig.25:a,b)

Stainless steel block of dimensions 29mm x 29mm x18mm with a cylindrical mold space of diameter 23mm and depth of 18mm were custom-made. Four holes each with a diameter of 3mm and depth of 18mm were drilled at the four corners of the block which were used to bolt it with the custom made positioning jig.

2. Preparation of Group I Test samples (Titanium abutments):

i) Attachment of Titanium abutments to implants: (Fig.26:a,b,c)

Ten titanium implants with standard platform, internal hexagon, tapered, 4.2 mm diameter, 10 mm length(NORIS Dental Implants) were used in the study. Ten Titanium abutments with 4.0 mm wide and 9 mm long were used. Each abutment was connected to these implants with the torque of 35 Ncm using a calibrated torque controller based on ISO 14801:2007 standard. In accordance

with this standard, the implant abutment torque within ± 5 % of the manufacturer's recommended value.

ii) Placement of implant abutment assembly in the stainless steel block:

(Fig:27,28)

The custom made stainless steel block was selected and placed on the surveying platform of a dental surveyor (Saeshin precision Ind Co., Korea) and stabilized. The surveying platform was made parallel to the floor using spirit level indicators (Jinhua Hengda Tools, China). **(Fig:27)** Then abutment connected to the implant was used as a carrier to orient the implant and it was attached to the surveying mandrel and positioned in the centre of the cylindrical space of the custom made stainless steel block such that implant was completely submerged in the cylindrical mold, except for 1mm at the crest of the module.

iii) Embedding procedure of implant abutment assembly with acrylic resin: (Fig:29,30)

Auto-polymerizing clear acrylic resin (Cold-cure, DPI, India) was mixed as per the manufacturers recommendations and poured in the mold space and then allow to polymerize. **(Fig:29)** This procedure was repeated to obtain 20 resin blocks. Reference points were marked in the resin blocks so that the abutments could be returned to the same position after each stage of testing. Another reference mark was placed on the abutments, where they emerged from the

implant and 90 ° from the mid labial point of loading. These marks acts as a positioning indicator during microscopic examination of the abutments (**Fig:30**).

3. Preparation of Group II Test samples (PEEK abutments):

i) Attachment of PEEK abutments to implants: (Fig.31:a,b)

Ten titanium implants with standard platform, internal hexagon, tapered, 4.2 mm diameter, 10 mm length(NORIS Dental Implants) were used in the study. Ten PEEK abutments with 4.0 mm wide and 9 mm long were used. Each abutment was connected to these implants with the torque of 35 Ncm using a calibrated torque controller based on ISO 14801:2007 standard. In accordance with this standard, the implant abutment torque within ± 5 % of the manufacturer's recommended value.

ii) Placement of implant abutment assembly in the stainless steel block:

(Fig:32)

The custom made stainless steel block was selected and placed on the surveying platform of a dental surveyor (Saeshin precision Ind Co., Korea) and stabilized. The surveying platform was made parallel to the floor using spirit level indicators (Jinhua Hengda Tools, China). (**Fig:27**) Then abutment connected to the implant was used as a carrier to orient the implant and it was attached to the surveying mandrel and positioned in the centre of the cylindrical space of the

custom made stainless steel block such that implant was completely submerged in the cylindrical mold, except for 1mm at the crest of the module. **(Fig:32)**

iii) Embedding procedure of implant abutment assembly with acrylic resin: (Fig:33,34)

Auto-polymerizing clear acrylic resin (Cold-cure, DPI, India) was mixed as per the manufacturers recommendations and poured in the mold space and then allow to polymerize. **(Fig:33)** This procedure was repeated to obtain 10 resin blocks. Reference points were marked in the resin blocks so that the abutments could be returned to the same position after each stage of testing. Another reference mark was placed on the abutments, where they emerged from the implant and 90° from the mid labial point of loading. These marks acts as a positioning indicator during microscopic examination of the abutments **(Fig:34)**.

4. Grouping of test samples: (Fig:35,36)

The embedded and numbered samples were assigned to two test groups based on the type of abutment. Group I test samples comprised of premachined titanium abutments connected to respective implants (NORIS Dental Implants) and they were labeled from GI 1 to GI 10 (n=10) **(Fig:31)**. Group II test samples comprised of PEEK abutments (NORIS Dental Implants) connected to their respective implants and they were labeled from GII 1 to GII 10 (n=10) **(Fig:32)**.

5. Quantitative and qualitative analysis of test samples before cyclic loading:

(Fig:37 A,B)

a. 3D Surface profilometry: (Fig:37A)

The test samples were subjected individually to 3D Surface profile scanning before cyclic loading. 3D Surface roughness was measured at the mid labial point of the abutment- implant interface with a reference point from where 90° point at implant- abutment interface using a 3D non-contact profilometer. The average surface roughness (Ra) value of each sample was obtained. The magnification of the optical lens was standardized at 50X for all the samples. Each sample was placed under the objective lens and resultant pictograph was obtained. This image was viewed as 3D and advanced 3D views using advanced aspheric analysis software.

b. Scanning Electron Microscope: (Fig:37B)

Each test sample was gold sputtered prior to SEM procedures to make the samples more electro conductive since SEM uses electrons and creates higher magnification and resolution images.

The implant abutment interface with reference to the mid labial point which was already marked at the platform from where the point is chosen at right angle was analysed by Scanning electron microscope S-3400N (Hitachi high technologies corporation, Japan) at 10 Kv acceleration voltages. Images are obtained at different magnification such that the implant abutment interface area

of each test sample could be visualized either completely under a lower magnification (30X) or a specific area could be visualized under suitable higher magnification(200X, 500X, 1000X) in separate images to aid in accurate measurement of the interface wear subsequently.

6. Fabrication of cement retained Ni-Cr cast crowns: (Fig:38 a,b,c,d,e)

Cement retained Ni-Cr single crowns of uniform dimensions for each of the Group I and Group II abutments

a) Preparation of wax pattern: (Fig:38 a)

One implant-abutment assembly was randomly selected from Group I. The abutment was coated with die lubricant (Yeti Dental, Germany) and excess lubricant was removed using a gentle stream of compressed air (Fig). Wax-up was done with inlay casting wax (GC Corporation, Tokyo, Japan) to obtain a single unit crown resembling a maxillary central incisor. The cingulum area was over contoured to create a flat surface at a 30° inclination to the long axis of the tooth.

b) Spruing, investing and burnout of wax pattern: (Fig:38 b,c)

Each wax pattern was sprued with a preformed wax sprue (REF 40085, Bego, Germany) of 2.5 mm diameter. The wax sprue was attached to the incisal edge of the pattern and a reservoir was placed 1.5 mm away from the pattern. The pattern was directly sprued to the crucible former of the ringless casting system (Sili Ring, Delta labs, Chennai, India). All the 20 wax patterns were sprued individually in a similar manner and invested individually using graphite free,

phosphate-bonded investment material (Bella sun, Bego, Germany) suitable for Ni-Cr alloy casting. The invested patterns were allowed to bench set for 20 minutes, and the silicone ring was removed and then allowed for 1 hour to set completely. Investments with the patterns for wax elimination were left in the burnout furnace (Technico, Technico laboratory products Pvt. Ltd., Chennai, India) for a period of three hours. The investment mold was initially placed in the furnace such that the crucible end was in contact with the floor of the furnace for the escape of molten material. The investment mold was reversed later near the end of burnout cycle with the sprue hole facing upward to enable escape of the entrapped gases and also to allow oxygen contact to ensure complete burnout of the wax pattern. The same procedure was followed for the burnout of all twenty patterns.

c) Casting, Divesting and Finishing the cast crowns: (Fig:38 d)

Casting was accomplished with Ni-Cr alloy (Bellabond plus, Bego, Germany) melted in an induction casting machine (Fornax, Bego, Germany). The casting procedure was performed quickly to prevent heat loss resulting in thermal contraction of the mold. The Ni-Cr alloy was heated to 1300⁰C according to manufacturers' recommendation for melting the alloy ingot and the crucible was released. The centrifugal force ensured the complete flow of the molten metal into the mold space. The same procedure was followed for casting all the twenty Ni-Cr crowns.

The hot casting was allowed to cool to room temperature. A knife was used to trim the investment at the bottom end of the ring. Adherent investment was removed from the casting by air abrasion using 110µm alumina (Korox, Chennai, India) at 80 psi pressure in a sand blasting machine (Delta labs, Chennai, India). Sprue was cut using a 0.7mm thin carborundum separating disc (Dentorium, New York, U.S.). The casting was inspected under magnification for casting defects. All the 20 cast crowns were trimmed using metal trimming burs (Edenta, Switzerland) and polished using silicon rubber wheels (DENTSPLY, Germany). Each finished crown was seated on its respective abutment and checked for proper fit and marginal accuracy.

7. Cementation of cement retained Ni-Cr cast crowns: (Fig:39,40)

Screw access should be blocked with cotton and a layer of wax before cementation. The cast restorations were then seated on the abutments. Cementation of these crowns were done using type I GIC (GC Corporation, Tokyo, Japan).

8. Cyclic loading of the test samples: (Fig:41)

The specimens with the cement retained cast restoration were attached to the loading platform of custom made loading machine (Lokesh Industries, Chennai) (ISO 7500-1 and ISO 4965) to simulate oral loading conditions at 30 degrees off-axis. This jig with the test sample was attached to the cyclic loading machine. The stylus of the cyclic loading machine was placed on the flattened

cingulum portion of the cast Ni-Cr central incisor crown. The test sample was subjected to cyclic loading. A sinusoidal waveform at 2Hz for load up to 200N (approximately) simulating human masticatory frequency and loads was applied. The angle of loading and applied force were representative of Class I anterior occlusion. This cycle was continued for 72hrs (with a break of 2hrs, every 21hrs) simulating 5,50,000 cycles which was approximately 1year of function. The sample cross checked for any damage for every 10 hours. The cyclic loading was performed in a dry environment. This procedure was repeated for all the twenty test samples.

9. Decementation of crown:

The restorations cemented over the abutments were removed by using metal cutting burs (SS WHITE GW-2) without damaging the abutments.

10. Quantitative and qualitative analysis of test samples after cyclic loading: (Fig:42A,B)

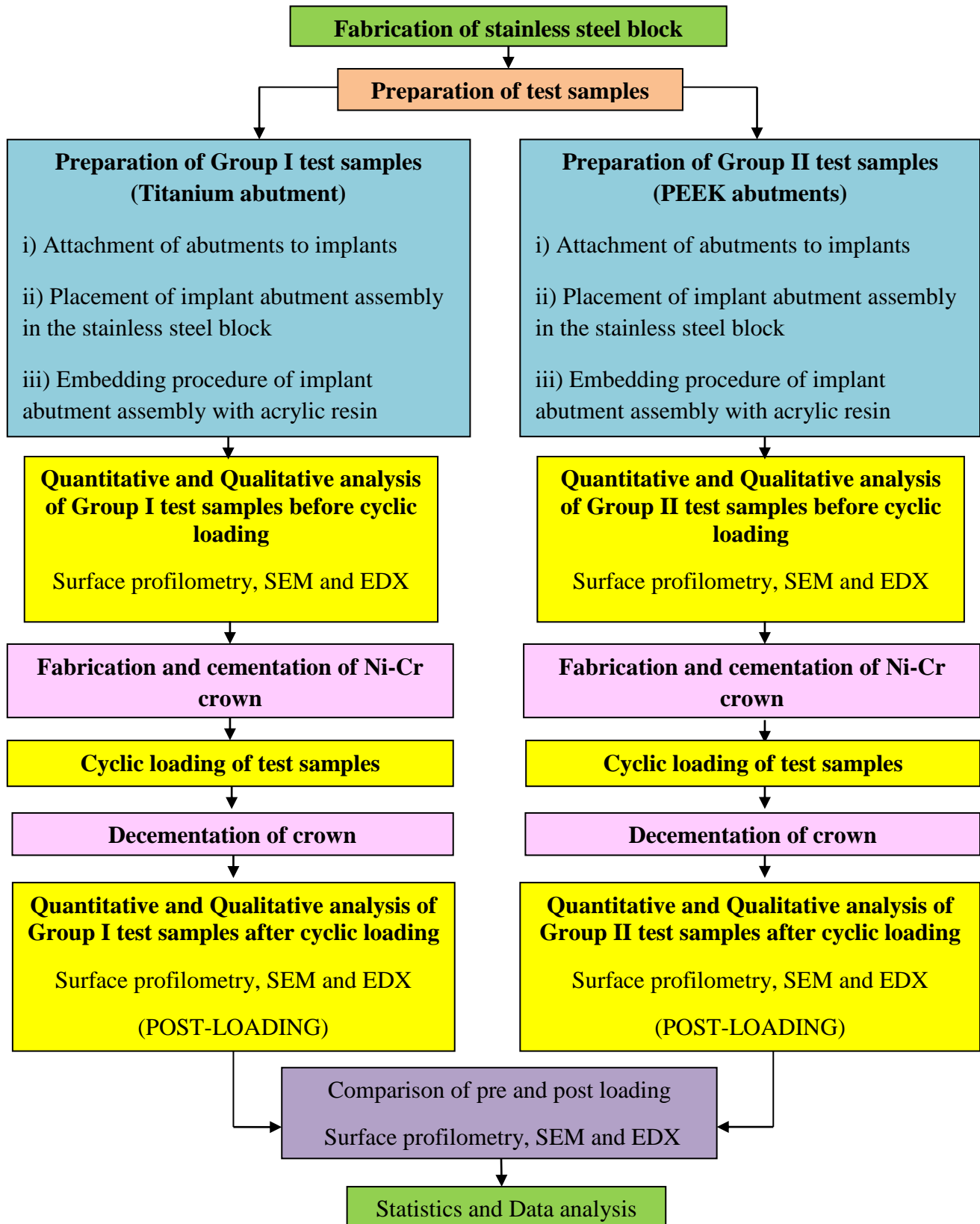
These abutment test samples were disconnected from the implants and visually inspected for any damage or deformation. Then again 3D Surface profilometry, Scanning electron microscopy and Energy dispersive X-Ray spectrophotometry were carried out as stated above for all the twenty abutment samples. After the cyclic loading with 5, 50,000 cycles the micrograph of the SEM shows striations caused by wear of abutment surface at the implant abutment interface.

11. Data tabulation and Statistical analysis:

The data obtained were tabulated using Microsoft excel and SPSS software. Paired 't' test was used to compare the mean pre and post cyclic loading Surface Roughness values within both test groups. Independent 't' test was used to compare the respective mean pre and post cyclic loading surface roughness values and the respective mean transverse difference between both the test groups.

ANNEXURE – I

METHODOLOGY OVERVIEW



ANNEXURE II

Calibration certificate for cyclic loading machine



Hi Tech Calibration Services

No. 130, Second Floor, VGP Nagar, Mugappair West, Chennai - 600 037

Phone : 044 - 2656 9696 / 2656 8696 / 4385 1234, Mobile : 98402 40996

Mail : enquiry@hitechcalibration.com, www.hitechcalibration.com

CALIBRATION CERTIFICATE				
Certificate No.	HT/456/001		Issue Date	5-Sep-2018
CUSTOMER DETAILS		TEST INSTRUMENT DETAILS		
Name	Dr. R. Maniamuthu,		Description	Cyclic Loading Machine
Address	Ragas Dental College, Utthandi, Chennai.		Make	--
			Range	--
			Leastcount	--
Job No	456		Mode	Compression
Job Date	4-Sep-2018		Serial No	1134006
Calibration done at	Site		Identification	--
Instrument Received Condition	Satisfied		Location	--
ENVIRONMENTAL CONDITION			Calibration On	4-Sep-2018
Temperature	25°C±5°C		Due On	3-Sep-2019
Humidity	35 %RH to 70%RH		Calibrated By	V.Prabu
STANDARD DETAILS				
Description	Load Cell with Indicator			
Certificate No.	SICC/CC/1195/11/2013-2014			
Valid Till	28-Nov-2018			
Traceability	SICC (NABL)			

CALIBRATION RESULT

Manual Mode :-

Max Load : 230.2 N

Min Load : 0.2 N

Auto Mode :-

Max Load : 225.8 N

Min Load : 0.2 N

Checked By
E.SALAJU - CALIBRATION ENGINEER
HT / PT / 538 / 01



Approved By
H.MENAKA - CALIBRATION ENGINEER

Page 1 of 1

ANNEXURE III

MATERIALS

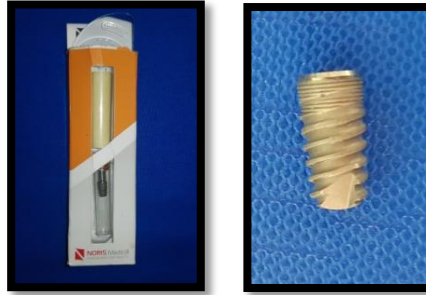


**Fig.1: Titanium dental implant standard platform
4.2mm diameter, 10 mm length (NORIS)**

a: Vial containing implant

b: NORIS dental implant



**Fig.2 : Premachined titanium abutment,
standard platform, internal hexagon**

a :Manufacturer packaging

b :Abutment



Fig.3: Pre machined PEEK abutment, standard platform, internal hexagon

a :Manufacturer packaging

b :Abutment

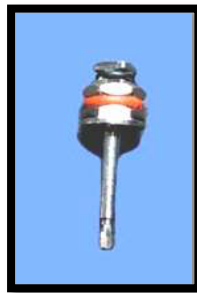


Fig.4: Hex driver



Fig.5:Torque wrench



Fig.6:Clear auto-polymerizing acrylic resin (RR Cold Cure., DPI, India)

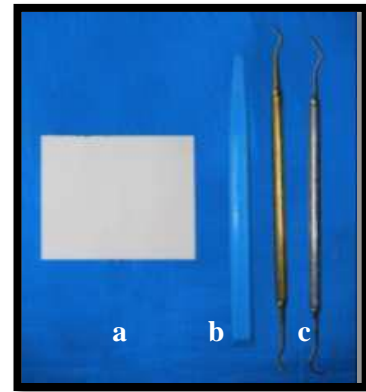
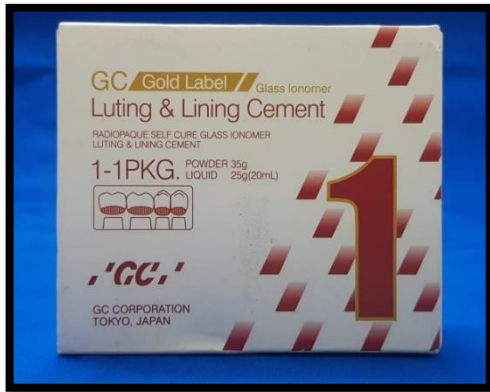


Fig.7 :Type I Glass Ionomer luting cement.

a :Mixing pad

b :Agate spatula

c :Plastic instrument



Fig.8: Die lubricant



Fig.9: Spirit level Indicators

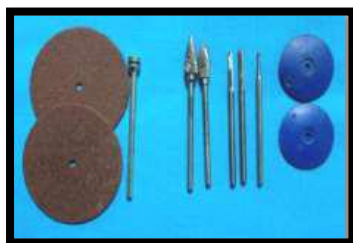


Fig.10: Burs



Fig.11: Inlay wax

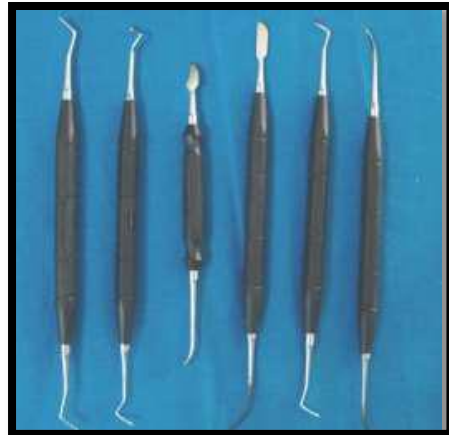


Fig.12: PKT Instruments



Fig.13a: Sprue wax
b: Silicone investment ring
c: Surfactant spray
d: Phosphate bonded investment material for Ni-Cr alloy
e: Colloidal silica



Fig.14: Ni-Cr metal pellets



Fig.15: Crucible former

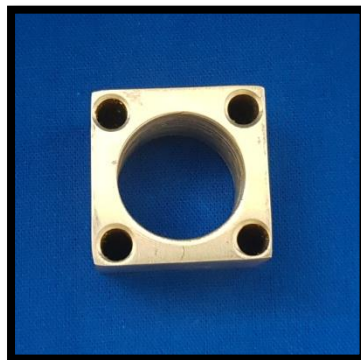


Fig.16: Stainless steel block



Fig.17: Dental Surveyor



Fig.18: Vacuum mixer



Fig.19: Burn out furnace



Fig.20: Casting Machine



Fig.21: Custom made Cyclic loading Machine



Fig.22: Custom made Positioning Jig

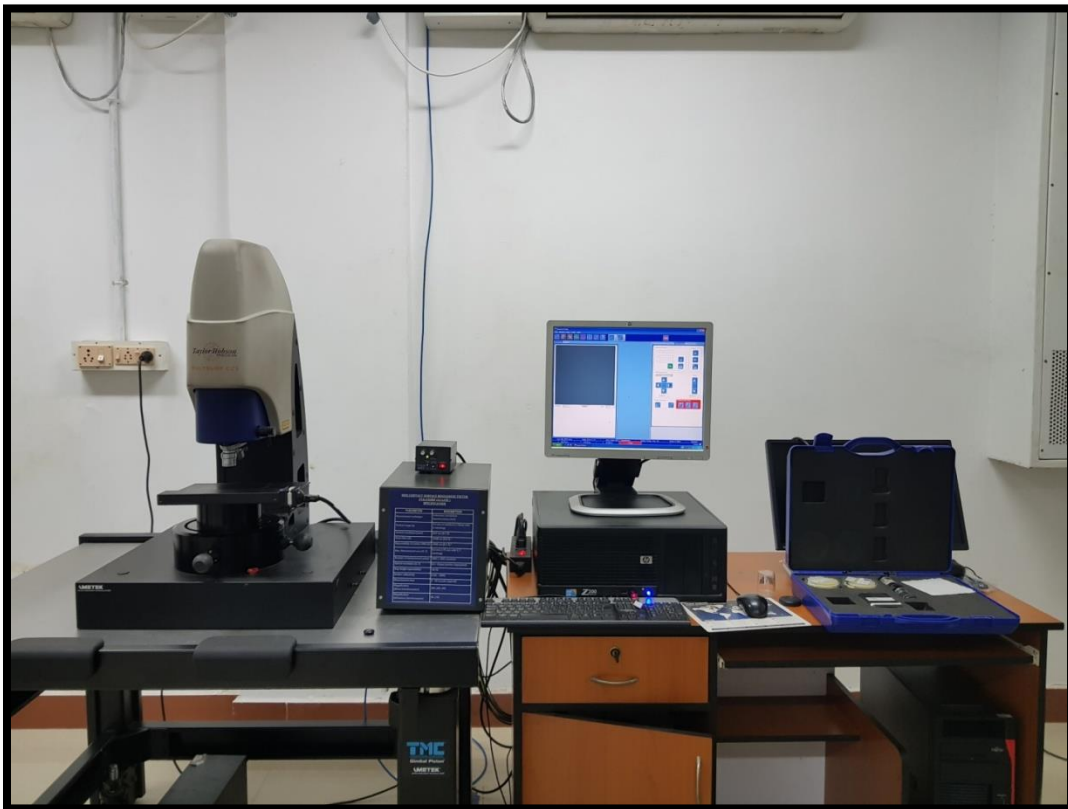


Fig.23: Surface Profilometer (Talysurf CCI Lite)



Fig.24: Scanning Electron Microscope S-3700N (Hitachi High Technologies Corporation, Japan)

METHODOLOGY

1. FABRICATION OF STAINLESS STEEL BLOCK

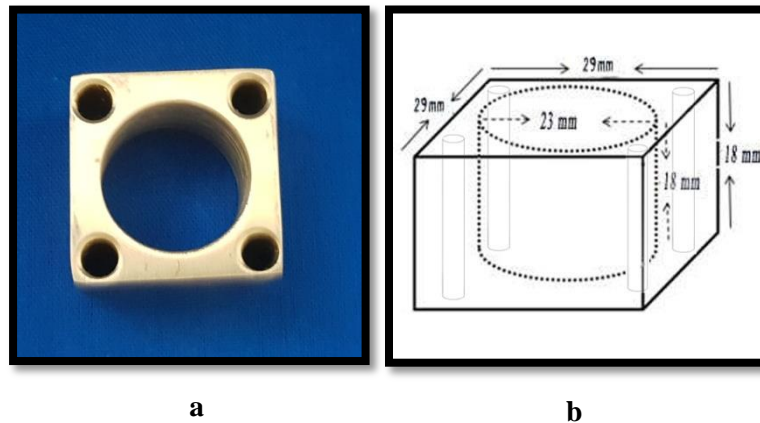


Fig.25: a. Stainless steel block

b. Line diagram of stainless steel block

2. PREPARATION OF GROUP I TEST SAMPLES (Titanium abutments)

i) Attachment of Titanium abutments to implants

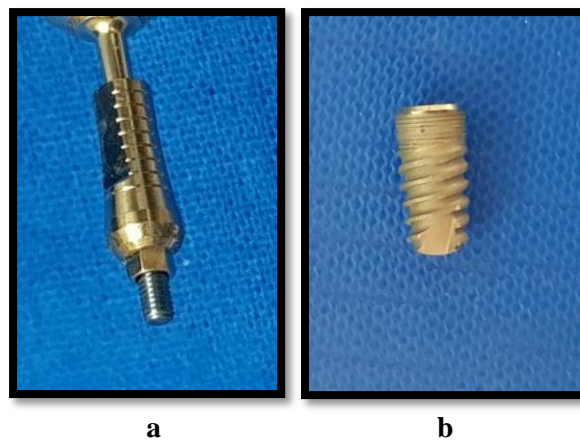


Fig.26: Connecting implant and abutments.

a. Titanium abutment

b. Titanium implant

ii) Placement of implant abutment assembly in the stainless steel block

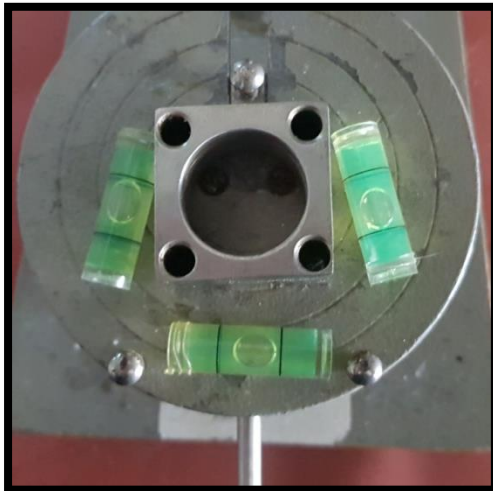


Fig.27: Paralleling the surveying platform with the spirit level indicators



Fig.28: Placing Titanium implant abutment assembly in the stainless steel block

iii) Embedding procedure of implant abutment assembly with acrylic resin

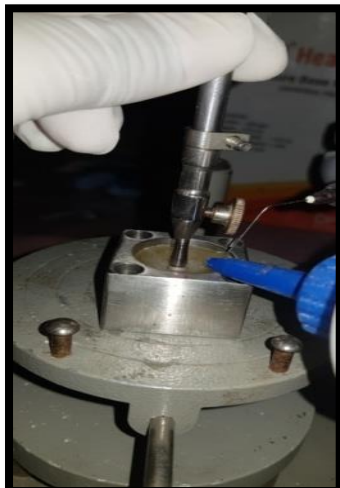


Fig.29: Placement of acrylic resin around the implant abutment assembly (Titanium)

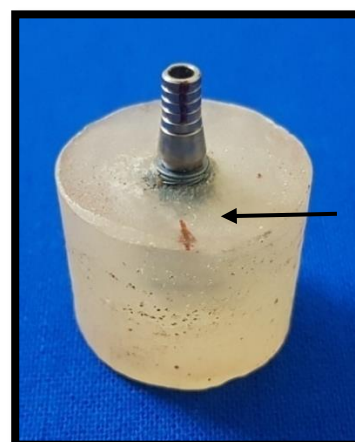


Fig.30: Mounted resin block with reference marks for orientation (Titanium)

3. PREPARATION OF GROUP II TEST SAMPLES (PEEK abutments)

i) Attachment of PEEK abutments to implants

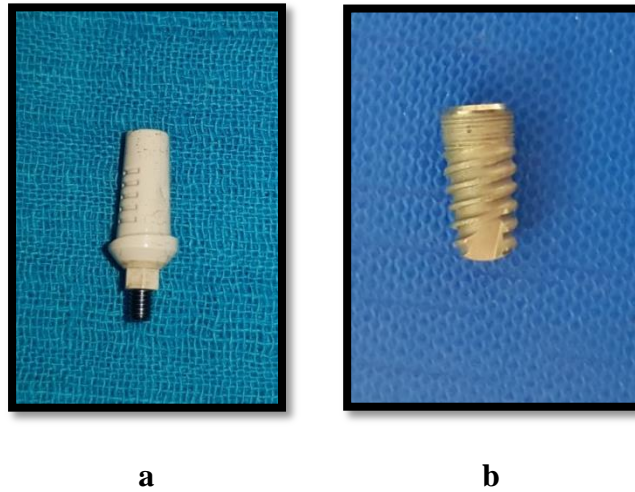


Fig.31: Connecting implant and abutments. (Group II)

a. PEEK abutment

b. Titanium implant

ii) Placement of implant abutment assembly in the stainless steel block

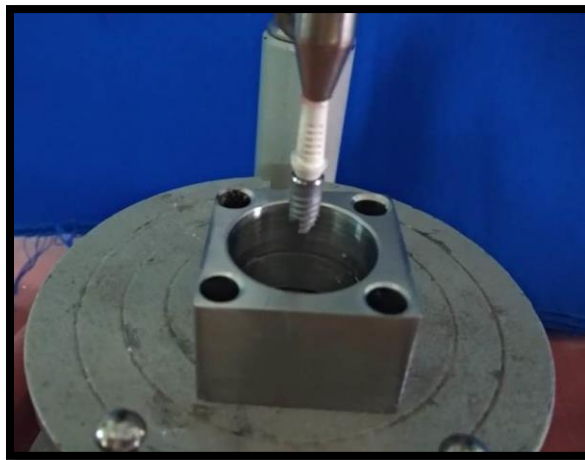


Fig.32: Placing implant and PEEK abutment assembly in the stainless steel block

iii) Embedding procedure of implant abutment assembly with acrylic resin



Fig.33: Placement of acrylic resin around the implant abutment assembly (PEEK abutment)

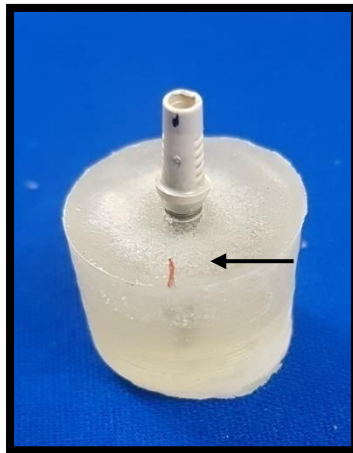


Fig.34: Mounted resin block with the reference marks for orientation (PEEK abutment)

4. Grouping of test samples

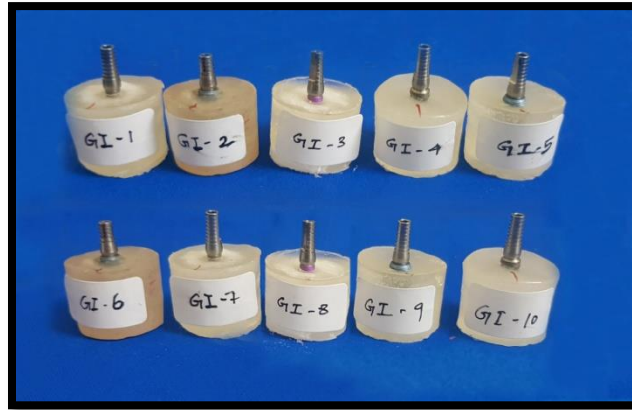


Fig.35: Group I Test samples (Implant-Abutment assembly with Titanium abutments)



Fig.36: Group II Test samples (Implant-Abutment assembly with PEEK abutments)

5. Quantitative and qualitative analysis of test samples before cyclic loading

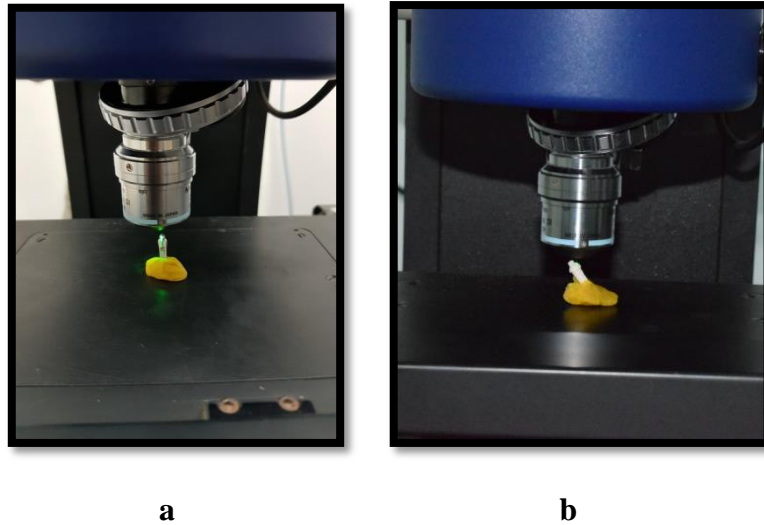


Fig.37A: Surface Profilometry done for analysis of surface roughness before loading

- a. Titanium abutment
- b. PEEK abutment

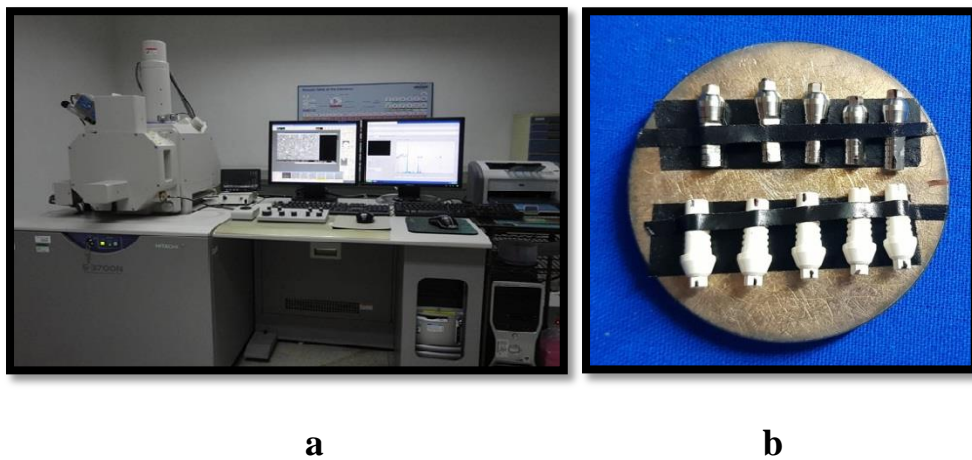


Fig.37B: Scanning electron microscopy before loading

- a. Microscope
- b. Samples

6. Fabrication of cement retained Ni-Cr cast crowns

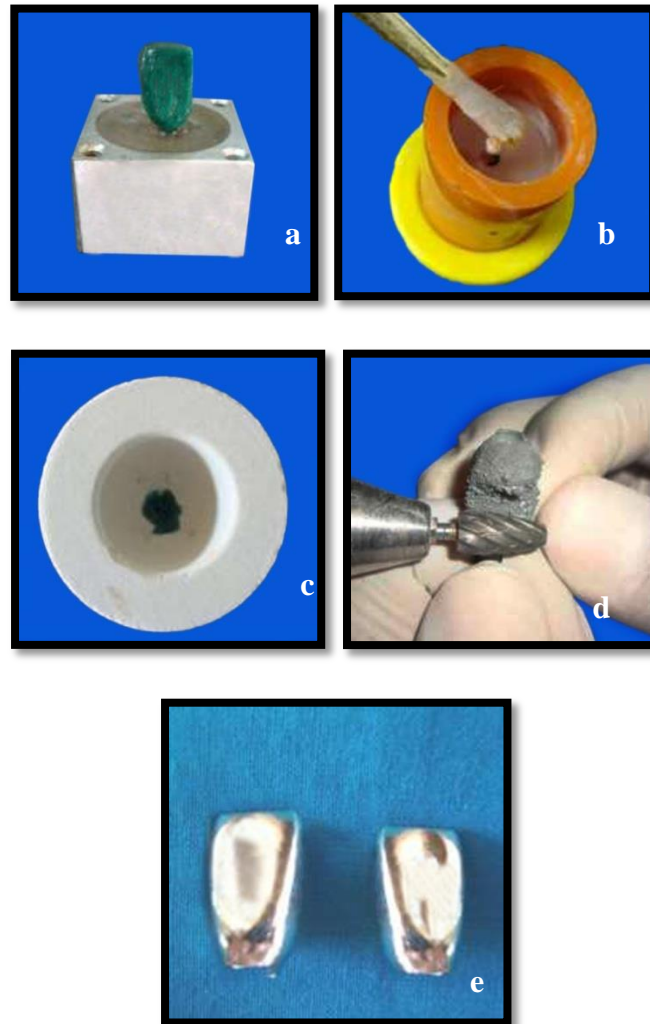


Fig.38: a. wax pattern preparation
b. Spruing and investing
c. Burnout and casting
d. Trimming and finishing the crowns
e. Finished Ni-Cr crowns

7. Cementation of Ni-Cr cast crowns

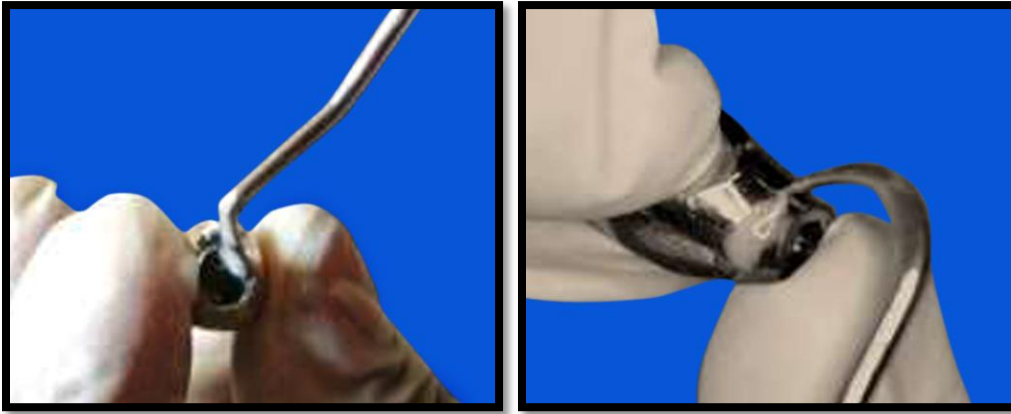


Fig.39: Group I Test samples with Ni-Cr crowns



Fig.40: Group II Test samples with Ni-Cr crowns

8. Cyclic loading of test samples



Fig.41: Cyclic loading

9. Quantitative and Qualitative analysis of test samples after cyclic loading

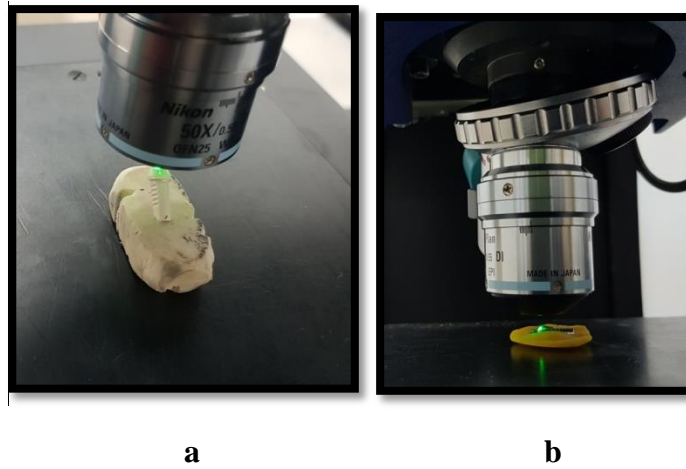


Fig.42A: Surface Profilometry done for analysis of surface roughness after loading

- a. Titanium abutment
- b. PEEK abutment

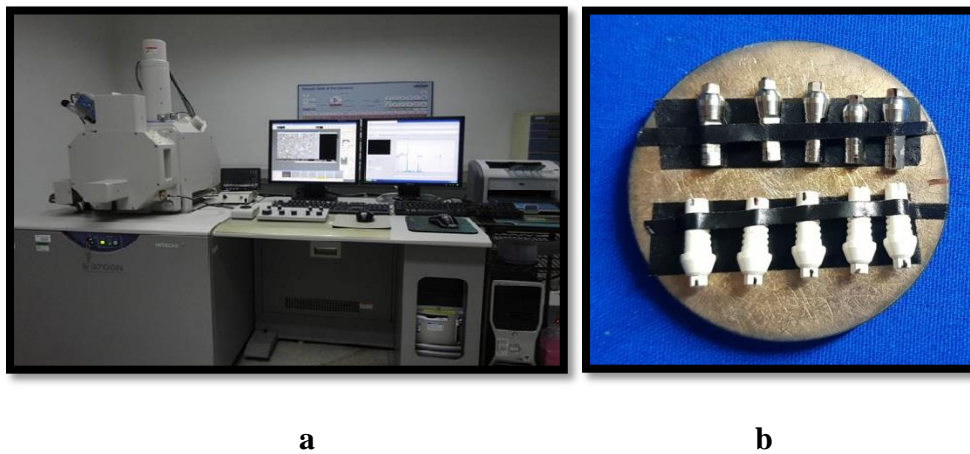


Fig.42B: Scanning electron microscopy after loading

- a. Microscope
- b. Samples

RESULTS

The Present in vitro study was conducted to evaluate the wear resistance of two different implant abutment materials after cyclic loading.

Ten Pre-machined Titanium straight abutments (GROUP I) and ten pre-machined PEEK straight abutments (GROUP II) were connected to their respective titanium implants which were then mounted in resin blocks. Qualitative and quantitative assessment of abutments at the implant abutment interface for both the groups were evaluated using Surface profilometry, Scanning Electron Microscopy and Energy Dispersive X-ray Spectrophotometry.

The cement retained Nickel chromium cast crowns were fabricated for all the abutments of both the groups. Abutments were torqued to 35 Ncm to their respective implants and crowns were cemented. The crowns were cyclically loaded upto 200 N for 5, 50,000 cycles, simulating 1 year usage. Crowns were removed and abutments were disconnected from the implants.

Then the implant abutment interface was again evaluated for surface roughness (Ra) values using Surface profilometer, Scanning electron microscope and Energy dispersive X-ray spectrophotometer. The basic and mean data of each test group was tabulated separately (Refer tables I-VI ; Graphs I-VI) and statistically analyzed using Paired't' test (Refer Tables VII and VIII ; Graphs VII and VIII) and Independent't' test (Refer Tables XI; Graphs XI). Qualitative assessment such as SEM micrographs and EDS results which are in line with the results of quantitative assessment were also added.

Table I: Basic and mean Pre-cyclic loading Surface roughness value (Pre Ra value₁) of Group I test samples (Pre-machined Titanium straight abutments)

Sample No.	Pre- Loading Surface Roughness (μm)
GI 1	0.381
GI 2	0.208
GI 3	0.499
GI 4	0.444
GI 5	0.338
GI 6	0.464
GI 7	0.314
GI 8	0.72
GI 9	0.387
GI 10	0.473
Mean/S.D	0.42/±0.14

Inference:

For Group I test samples, the maximum pre-cyclic loading Surface Roughness value was 0.72μm and the minimum precyclic loading Surface roughness value was 0.208μm. The mean pre cyclic loading Surface roughness value was 0.42μm.

Table II: Basic and mean Post-cyclic loading Surface roughness value (Post Ra value₁) of Group I test samples (Pre-machined Titanium straight abutments)

Sample No.	Post- Loading Surface Roughness (μm)
GI 1	0.366
GI 2	0.468
GI 3	0.442
GI 4	0.509
GI 5	0.416
GI 6	0.378
GI 7	0.689
GI 8	0.782
GI 9	0.403
GI 10	0.501
Mean/S.D	0.495/0.14

Inference:

For Group I test samples, the maximum Post-cyclic loading Surface Roughness value was 0.782μm and the minimum post-cyclic loading Surface roughness value was 0.366μm. The mean post-cyclic loading Surface roughness value was 0.495μm.

Table III: Basic and mean Surface roughness difference value (Ra value D₁) of Group I test samples (Pre-machined Titanium straight abutments)

Sample No.	Pre- Loading Surface Roughness (μm)	Post- Loading Surface Roughness (μm)	Difference (μm)
GI 1	0.381	0.366	0.015
GI 2	0.208	0.468	-0.26
GI 3	0.499	0.442	0.057
GI 4	0.444	0.509	-0.065
GI 5	0.338	0.416	-0.078
GI 6	0.464	0.378	0.086
GI 7	0.314	0.689	-0.375
GI 8	0.72	0.782	-0.062
GI 9	0.387	0.403	-0.016
GI 10	0.473	0.501	-0.028
Mean/S.D	0.42/±0.14	0.495/0.14	-.073/0.142

Inference:

For Group I test samples, the maximum Surface Roughness (Ra value) difference was 0.086 μm and the minimum Surface roughness (Ra value) difference was -0.375 μm. The mean Surface roughness difference value of Group I samples was -0.073 μm.

Table IV: Basic and mean Pre-cyclic loading Surface roughness value (Pre Ra value₂) of Group II test samples (Pre-machined PEEK straight abutments)

Sample No.	Pre- Loading Surface Roughness (μm)
GII 1	3.752
GII 2	0.366
GII 3	0.17
GII 4	0.118
GII 5	0.15
GII 6	0.321
GII 7	0.173
GII 8	0.11
GII 9	0.197
GII 10	0.346
Mean/S.D	0.23/0.10

Inference:

For Group II test samples, the maximum pre-cyclic loading Surface Roughness value was 3.752μm and the minimum pre-cyclic loading Surface roughness value was 0.11μm. The mean pre-cyclic loading Surface roughness value was 0.23μm

Table V: Basic and mean Post-cyclic loading Surface roughness value (Post Ra value₂) of Group II test samples (Pre-machined PEEK straight abutments)

Sample No.	Post- Loading Surface Roughness (μm)
GII 1	0.394
GII 2	0.277
GII 3	0.159
GII 4	0.186
GII 5	0.15
GII 6	0.315
GII 7	0.321
GII 8	0.174
GII 9	0.125
GII 10	0.211
Mean/S.D	0.233/0.091

Inference:

For Group II test samples, the maximum Post-cyclic loading Surface Roughness value was 0.321μm and the minimum Post-cyclic loading Surface roughness value was 0.15μm. The mean Post-cyclic loading Surface roughness value was 0.233μm.

Table VI: Basic and mean Surface roughness difference value (Ra value D₂) of Group II test samples (Pre-machined PEEK straight abutments)

Sample No.	Pre- Loading Surface Roughness (μm)	Post- Loading Surface Roughness (μm)	Difference (μm)
GII 1	3.752	0.394	3.358
GII 2	0.366	0.277	0.089
GII 3	0.17	0.159	0.011
GII 4	0.118	0.186	-0.068
GII 5	0.15	0.15	0
GII 6	0.321	0.315	0.006
GII 7	0.173	0.321	-0.148
GII 8	0.11	0.174	-0.064
GII 9	0.197	0.125	0.072
GII 10	0.346	0.211	0.135
Mean/S.D	0.23/0.10	0.233/0.091	-.0004/0.04

Inference:

For Group II test samples, the maximum Surface Roughness (Ra value) difference was 0.135 μm and the minimum Surface roughness (Ra value) difference was -0.148 μm. The mean Surface roughness (Ra value) difference value of Group II was -0.0004 μm.

Table VII: Comparative evaluation of the mean pre-cyclic loading and post cyclic loading surface roughness values for Group I test samples (Pre-machined Titanium straight abutments)

GROUP I ((Pre-machined Titanium straight abutments)	Number of samples	Mean Surface Roughness value (Ra) (μm)	p- value
Pre Loading	10	0.422800	0.140
Post Loading	10	0.495400	

p-value is 0.140; insignificant at 5 level

Inference:

On comparison using Paired ‘t’ test, it was found that the mean post-cyclic loading Surface Roughness (Ra) Value of Group I test samples was higher than the mean pre-cyclic loading Surface Roughness (Ra) Value and this was found to be statistically insignificant. (p value is 0.140)

Table VIII: Comparative evaluation of the mean pre-cyclic loading and post cyclic loading surface roughness values for Group II test samples (Pre-machined PEEK straight abutments)

GROUP II ((Pre-machined PEEK straight abutments)	Number of samples	Mean Surface Roughness value (Ra) (μm)	p- value
Pre Loading	10	.232620	0.976
Post Loading	10	.233000	

p-value is 0.976; Insignificant at 5 level

Inference:

On comparison using Paired 't' test, it was found that the mean post-cyclic loading Surface Roughness (Ra) Value of Group II test samples was same as the mean pre-cyclic loading Surface Roughness (Ra) Value and this was found to be statistically insignificant. (p value is 0.976)

Table IX: Comparative evaluation of the mean difference values of pre and post- cyclic loading Surface roughness (Ra value) of Group I (Pre-machined Titanium straight abutments) and Group II test samples (Pre-machined PEEK straight abutments)

GROUP	Number of samples	Mean Surface Roughness value (Ra) (μm)	Standard deviation	p- value
I Surface roughness(Ra) value	10	-.072600	.1420408	0.272
II Surface roughness(Ra) value	10	-.000380	.0387657	

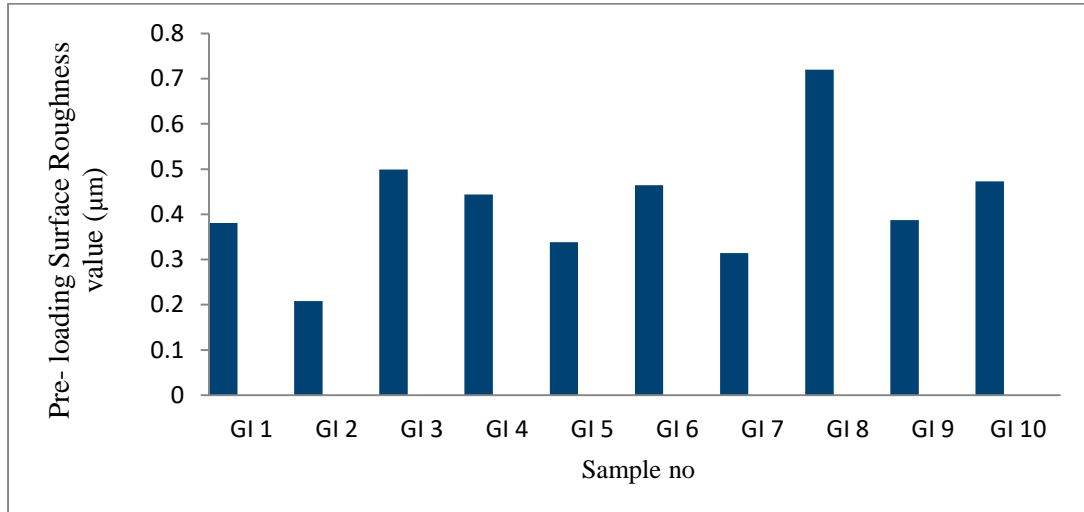
p- value is 0.272, insignificant at 5 level

Inference:

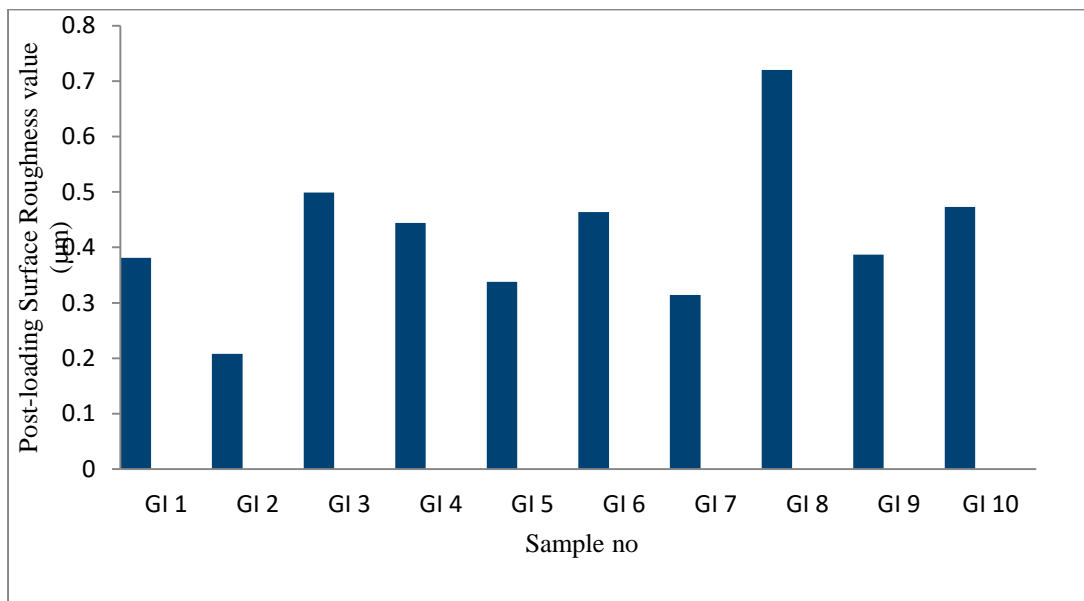
On comparison using Independent ‘t’ test, it was found that the mean difference values of pre and post- cyclic loading Surface roughness (Ra value) of Group I (Pre-machined Titanium straight abutments) was lower than the Group II test samples (Pre-machined PEEK straight abutments) and this was found to be statistically insignificant. (p value is 0.272)

ANNEXURE-IV

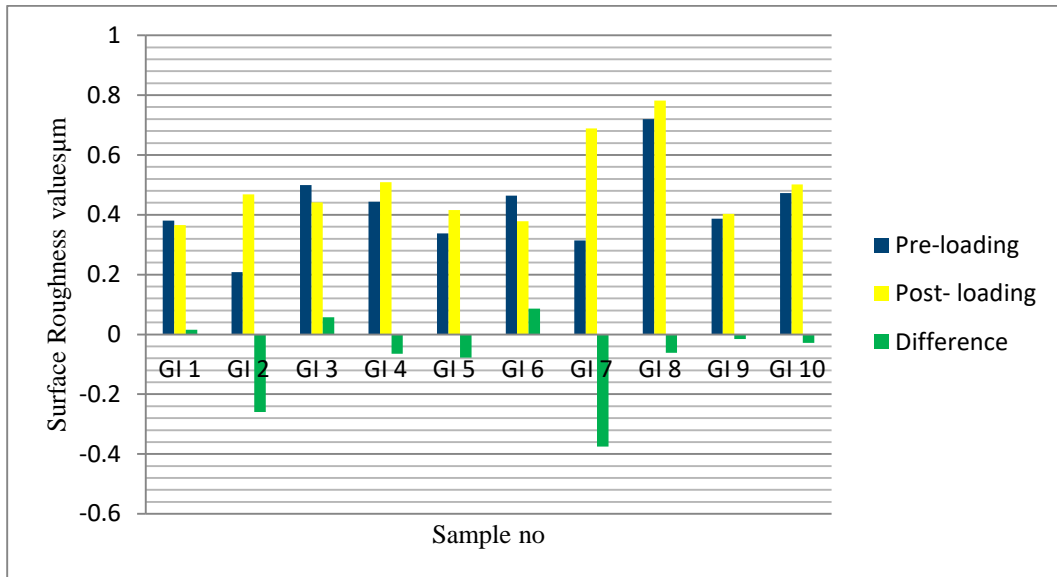
Graph I: Basic pre-cyclic loading Surface roughness values (Pre Ra value₁) of Group I test samples (Titanium pre-machined straight abutments)



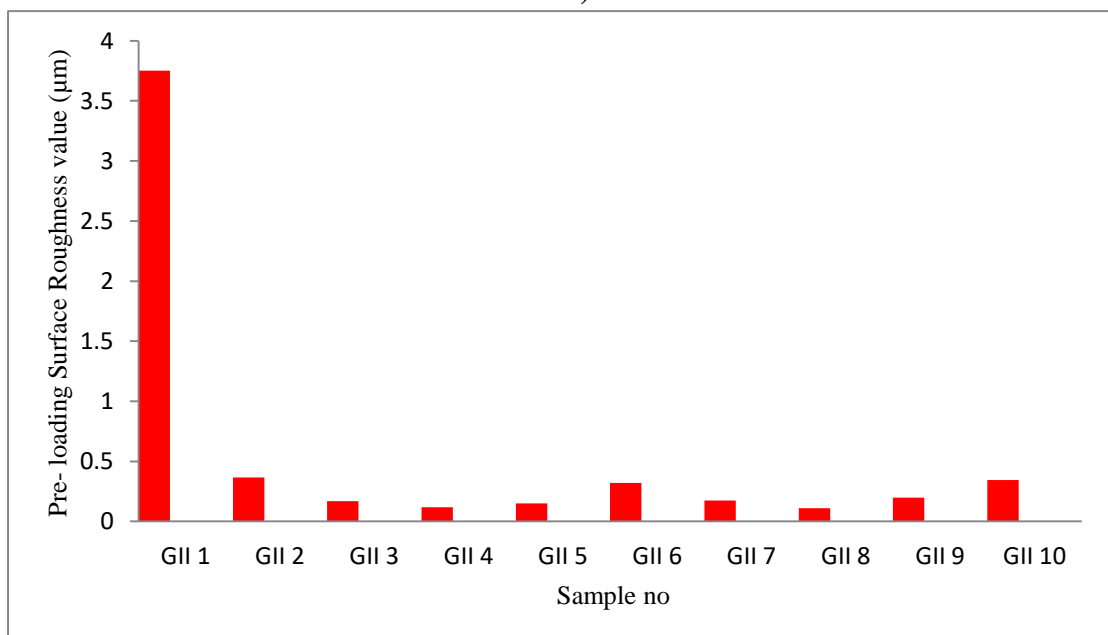
Graph II: Basic Post-cyclic loading Surface roughness values (Post Ra value₁) of Group I test samples (Titanium pre-machined straight abutments)



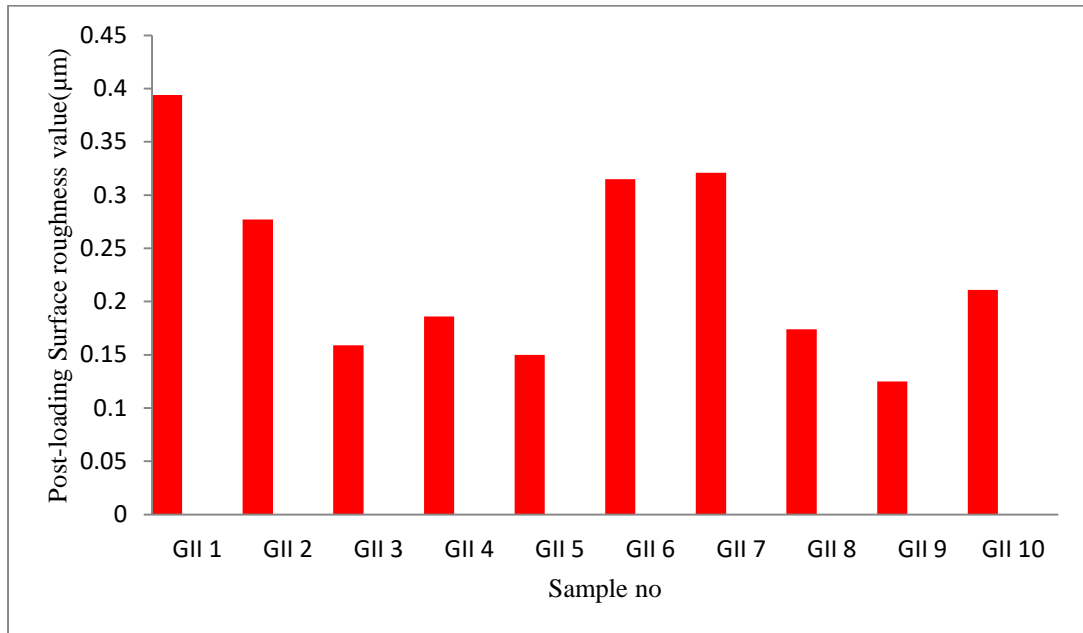
Graph III: Basic Pre and Post loading Surface roughness (Ra value D₁) differences of Group I test samples (Titanium pre-machined straight abutments)



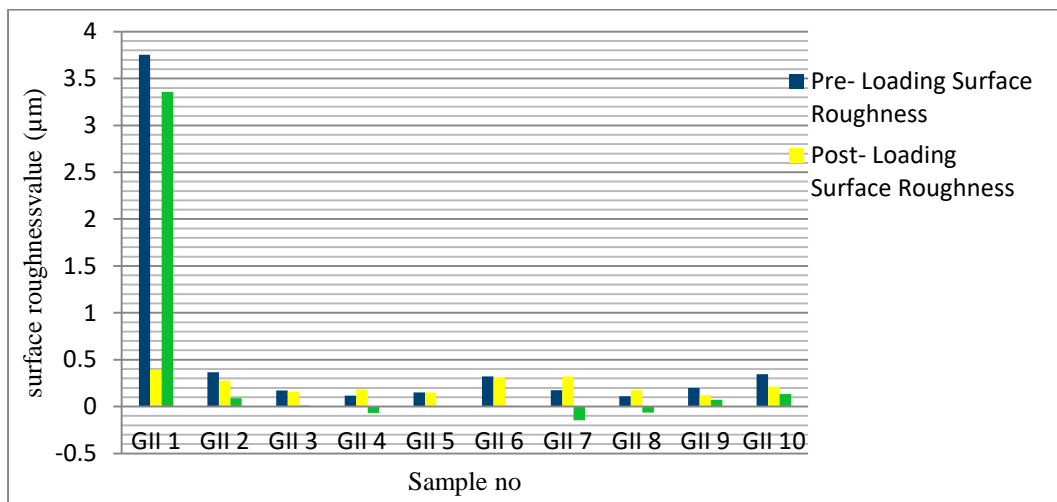
Graph IV: Basic pre-cyclic loading Surface roughness values(Pre Ra value₂) of Group II test samples (Pre- machined PEEK straight abutments)



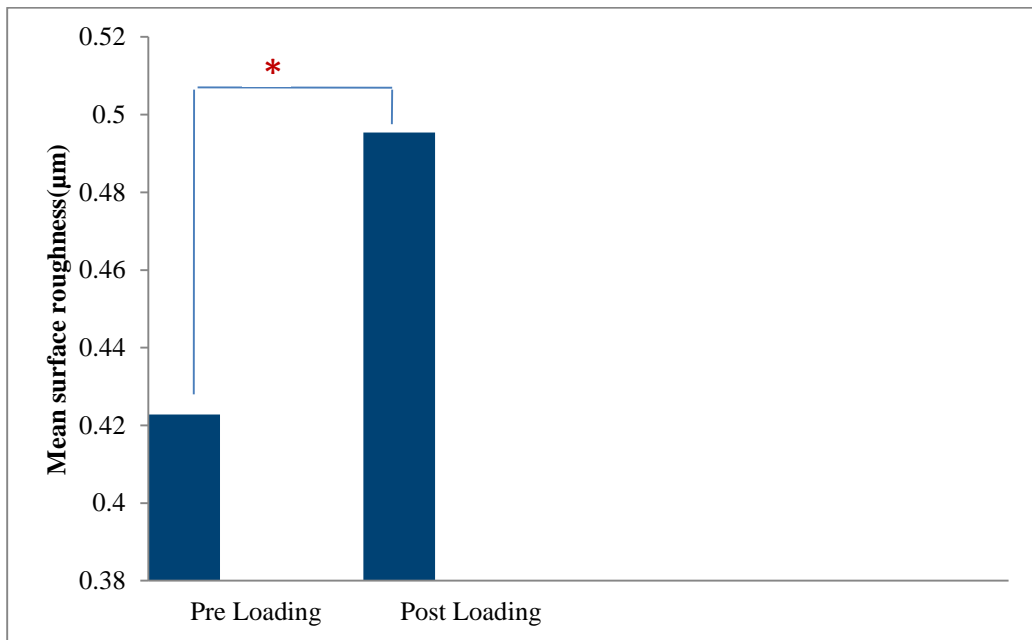
Graph V: Basic Post-cyclic loading Surface roughness values (Post Ra value₂) of Group II test samples (PEEK pre-machined straight abutments)



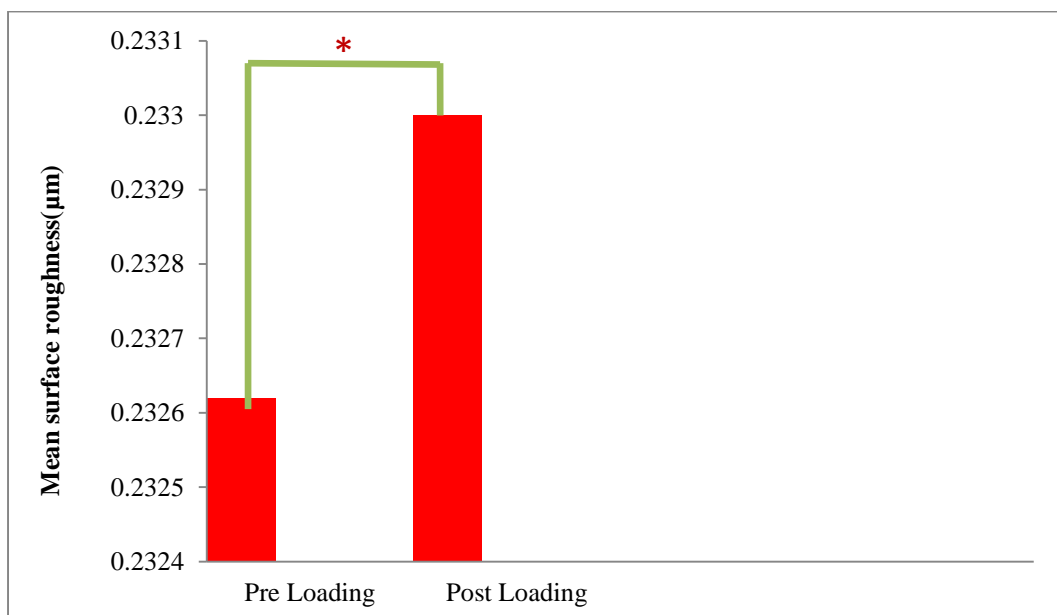
Graph VI: Basic pre and post-cyclic loading Surface roughness difference values (Ra value D₂) of Group II test samples (PEEK pre-machined straight abutments)



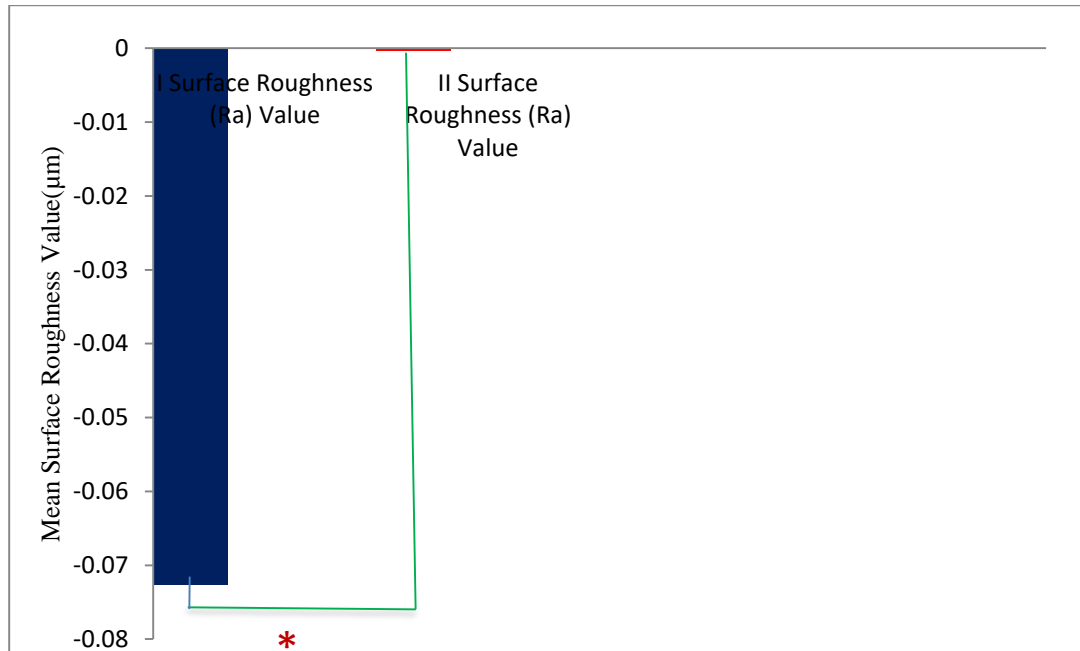
Graph VII: Comparative evaluation of the mean pre and post- cyclic loading Surface roughness (Ra value) values of Group I test samples (Pre-machined Titanium straight abutments)



Graph VIII: Comparative evaluation of the mean pre and post- cyclic loading Surface roughness (Ra value) values of Group II test samples (Pre-machined PEEK straight abutments)



Graph IX: Comparative evaluation of the mean pre and post- cyclic loading Surface roughness (Ra value) of Group I (Pre-machined Titanium straight abutments) and Group II test samples (Pre-machined PEEK straight abutments)



3D SURFACE TEXTURE PHOTOMICROGRAPHY

GROUP II TEST SAMPLE

(PEEK abutment Pre-cyclic loading)

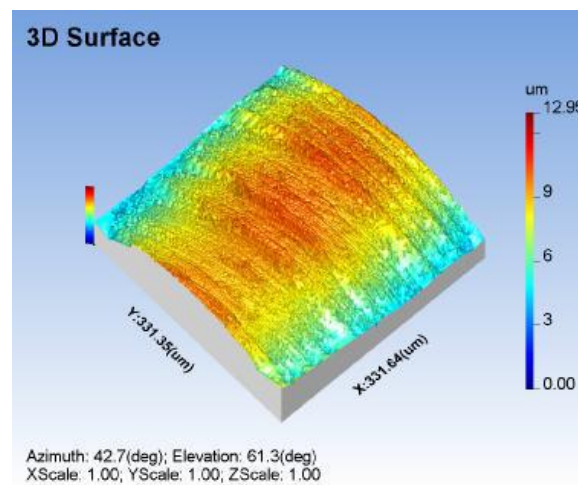


Fig.45: Advanced 3D view of surface topography of Group II (PEEK Abutment) before cyclic loading

Inference :

3D view of surface topography of Group II test sample before cyclic loading revealed micro striated irregularities under 50x

3D SURFACE TEXTURE PHOTOMICROGRAPHY

GROUP II TEST SAMPLE

(PEEK abutment Post-cyclic loading)

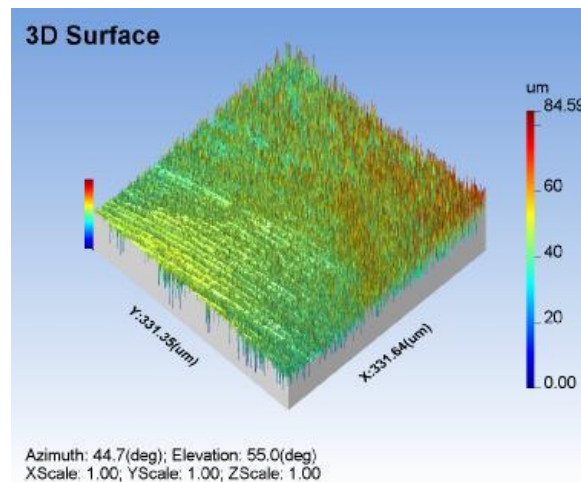


Fig.46: Advanced 3D view of surface topography of Group II (PEEK Abutment) after cyclic loading

Inference :

3D view surface topography of Group II test sample after cyclic loading revealed increased micro striated irregularities under 50x represented by peaks and valleys

ANNEXURE - V

3D SURFACE TEXTURE PHOTOMICROGRAPHY

GROUP I TEST SAMPLE

(Titanium abutment Pre-cyclic loading)

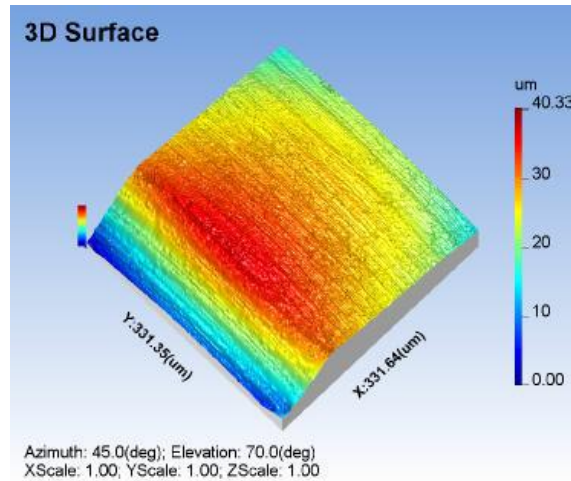


Fig. 43: Advanced 3D view of surface topography of Group I (Titanium Abutment) before cyclic loading

Inference :

3D view surface topography of Group I test sample before cyclic loading revealed coarse striations and irregularities under 50x indicates rough surface.

3D SURFACE TEXTURE PHOTOMICROGRAPHY

GROUP I TEST SAMPLE

(Titanium abutment Post-cyclic loading)

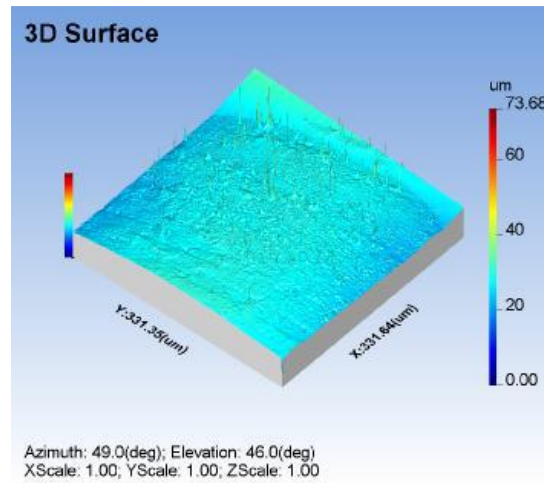


Fig.44: Advanced 3D view of surface topography of Group I (Titanium Abutment) after cyclic loading

Inference :

3D view surface topography of Group I test sample after cyclic loading revealed micro irregularities and diminution of voids under 50x indicating wear in the rough surface.

SEM MICROGRAPHS
GROUP II TEST SAMPLE
(PEEK abutment Pre loading)

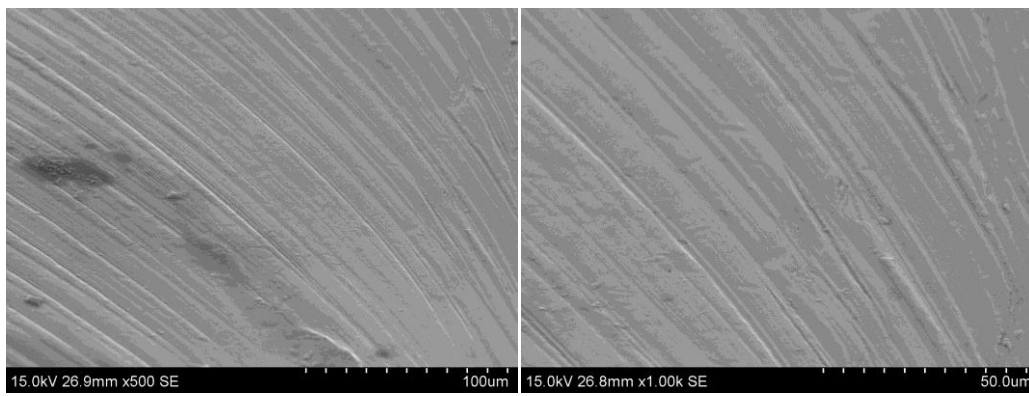


Fig.49 :SEM micrographs at magnifications 500X and 1000X shows surface with less irregularities before cyclic loading of Group II test samples respectively

Inference :

SEM micrograph of Group II test sample before cyclic loading revealed micro striated irregularities under 500x and at 1000x it appeared as sparsely distributed striations indicating smoother surface.

SEM MICROGRAPHS
GROUP II TEST SAMPLE
(PEEK abutment Post loading)

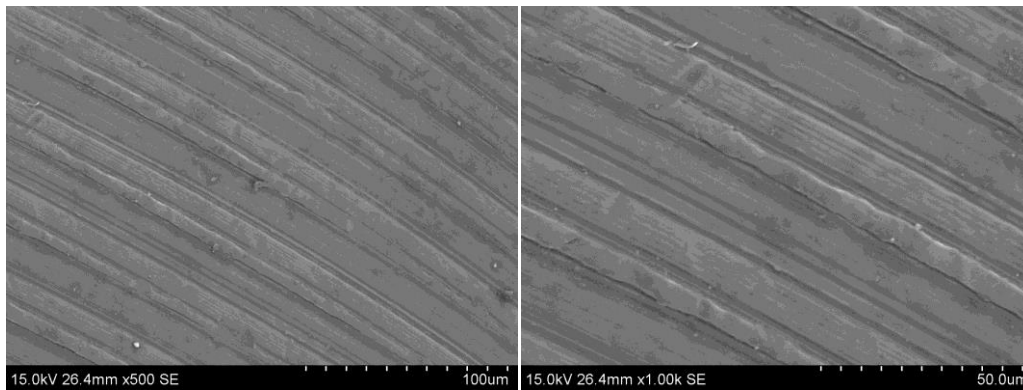


Fig.50: SEM micrographs at magnifications 500X and 1000X shows surface with increased irregularities after cyclic loading of Group II test samples

Inference:

SEM micrograph of Group II test sample after cyclic loading revealed increased micro striated irregularities under 500x and at 1000x it appeared as sparsely distributed striations indicating changes in surface topography

ANNEXURE-VI
SEM MICROGRAPHS
GROUP I TEST SAMPLE
(Titanium abutment Pre loading)

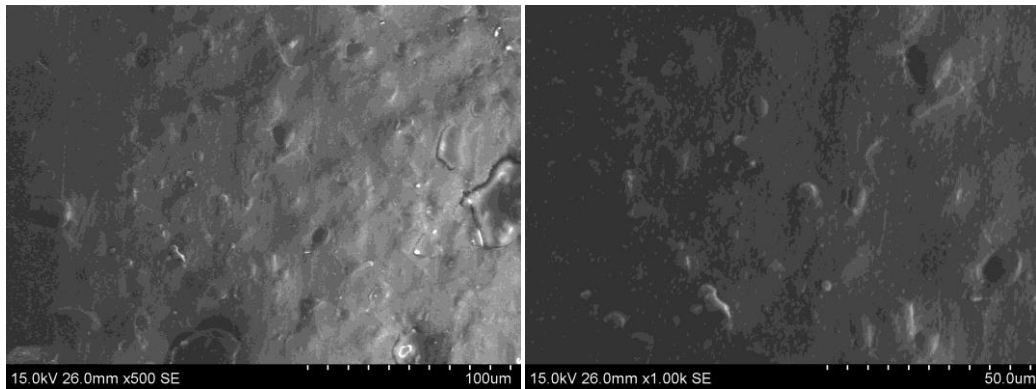


Fig.47 :SEM micrographs at magnifications 500X and 1000X shows surface with presence of voids and irregularities before cyclic loading of Group I test samples

Inference:

SEM micrograph of Group I test sample before cyclic loading revealed patchy irregularities and presence of voids under 500x and at 1000x it appeared as sparsely distributed voids and indicating rough surface.

SEM MICROGRAPHS
GROUP I TEST SAMPLE
(Titanium abutment Post loading)

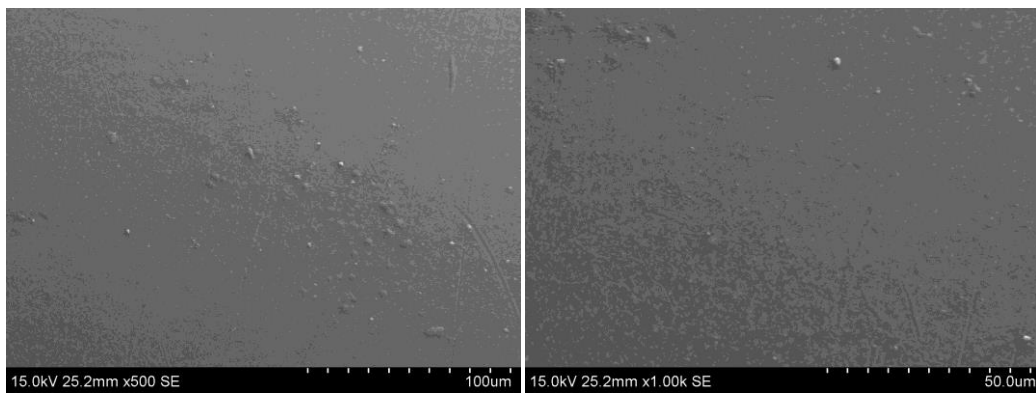


Fig.48 :SEM micrographs at magnifications 500X and 1000X shows surface with diminished voids and reduction in irregularities representing wear after cyclic loading of Group I test samples

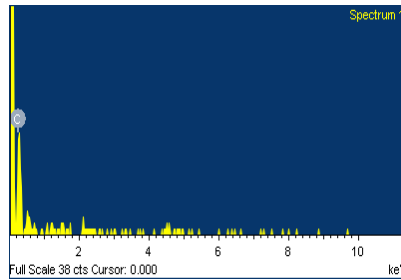
Inference :

SEM micrograph of Group I test sample after cyclic loading revealed micro irregularities and diminution of voids under 500x and at 1000x it appeared as sparsely distributed diminished voids indicating wear in the rough surface.

ENERGY DISPERSIVE X-RAY SPECTROPHOTOMETRY

GROUP II TEST SAMPLE

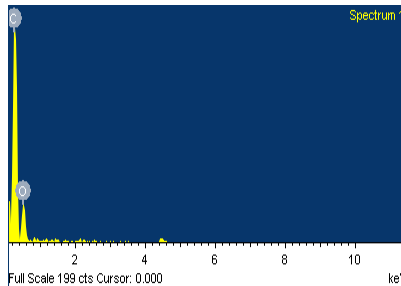
PEEK Pre-cyclic loading



Inference:

EDS results of PEEK before loading indicates the presence of 100% Carbon.

PEEK Post cyclic loading

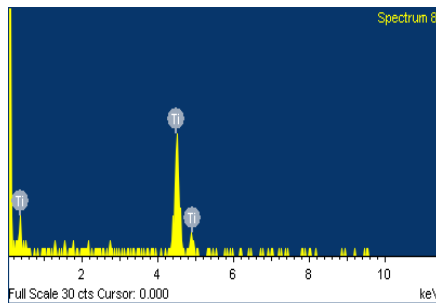


Inference:

EDS results of PEEK after loading indicates the presence of 66.04% Carbon and 33.96% Oxygen.

ANNEXURE – VII
ENERGY DISPERSIVE X-RAY SPECTROPHOTOMETRY
GROUP I TEST SAMPLE

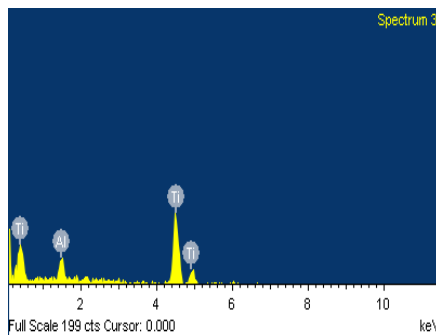
Titanium abutment Pre loading



Inference:

EDS results of Titanium abutment before loading indicates the presence of 100% Titanium.

Titanium abutment Post- loading



Inference:

EDS results of titanium abutment after loading indicates the presence of 16.36% Aluminium and 83.94% Titanium.

DISCUSSION

The present in vitro study was conducted to comparatively evaluate wear resistance of two different implant abutment materials after cyclic loading.

Implant dentistry has become a trend and going through significant developments in past decades. Traditionally, implant supported restorations were introduced for restoration of completely edentulous arches. But, now the continued evolution of materials, techniques and their usage expanded the indication spectrum to partially edentulous and also single tooth restorations.^{1,4,11,24}

Likewise the success criteria for the implant restorations were believed to be the osseointegration then the focus has gradually changed and included a variety of mechanical and esthetic challenges. Mechanically there should be healthy, harmonious and maintainable interface between the implant supported restorations and the peri implant tissues. Aesthetically, the parameters considered are color and shape of restoration; topography and appearance of soft tissues.^{5,7,19}

In conventional implant restorations, the most important factor is design, color and material of an implant abutment which represents the transmucosal connection between the implant and its superstructure.^{13,19,24,34} The mating surfaces of the implant and its abutment form the implant abutment interface and is considered to be a crucial aspect of the implant design.^{4,6,16}

The design of the fitting surfaces of the abutment will influence the precise fit of the implant and abutment. Implant abutment connections determines the prosthetic stability by transferring the stress created by the loading forces and providing a microbial seal.^{4,6,8,38,41}

The type of abutment material used also has a vital role in the quality of attachments of mucosa and implants. A material to be used as an abutment should have ideal physical properties such as elastic modulus and strength to withstand the occlusal forces without permanent deformation. Regarding the elastic modulus, the abutment material should have yield strength as closely related to the bone as possible for better stress distribution.^{5,16,17,22,23,39,44}

A study conducted by Truninger et al⁴⁹ also demonstrated that both the abutment material and type of connection influences the bending moments of abutments after aging and chewing simulation.⁴⁹

Considering these factors, commercially pure titanium had been used as a standard material for the implants and abutments traditionally. Titanium exhibits good biocompatibility, corrosion resistance and it is highly reactive and rapidly form a tenacious oxide layer that is responsible for the metal's biocompatibility.^{6,19,53,49} Even though, Titanium and its alloys has good biocompatibility, ability to overcome mechanical challenges, esthetically, in thin gingival biotype appearance of grayish discoloration at the cervical margin, makes

it unacceptable and due to its high elastic modulus (104 GPa) when compared to human bone (3 GPa) instead of absorbing the masticatory forces, titanium transfers these forces to adjacent bone that leads to stress shielding which may cause bone resorption and fracture at the area of implant abutment connection. However, for esthetic reasons and stress shielding effects materials different from titanium were used.^{31,32,35}

Nowadays, to overcome the esthetic challenges, the trend is towards the use of non metal tooth colored materials such as ceramics and polymers as abutments, which benefits for esthetics, biomechanics and easy processing methods.¹⁹

Ceramics such as alumina and zirconia were used for abutment manufacturing, in which alumina exhibited lower fracture resistance but zirconia is harder than alumina and substituted titanium in esthetic areas. The main disadvantages of zirconia were their brittleness, additional bulk of porcelain should be added in need of low shade, aging and sensitivity to temperature.^{22,23,36,45,47}

As there is less resilience at the implant bone interface due to decrease in proprioception directly affects the stress distribution sometimes lead to excessive stress on restoration and chipping of porcelain which is a common problem for

implant supported restorations with either metal or zirconia core. Therefore, stress concentrations should be avoided.^{13,16,19,31}

Resin based restorative materials may reduce the stress on implants and peripheral bone. Currently, the PEEK biomaterial gained its attention which was earlier used as provisional abutments. These abutments used to create a gingival contour during temporary restoration period.

In a previous study conducted by Koutouzis et al²⁴ showed that there is no significant difference in the bone resorption and soft tissue inflammation around PEEK and titanium abutments and a significant difference was observed that, PEEK provisional abutments showed lesser plaque accumulation than titanium provisional abutments even though the surface roughness of PEEK is high.^{31,33,40}

PEEK has very high mechanical resiliency and resistant to corrosion and also has shock absorption properties. Due to its excellent chemical stability, resistance to radiation used in sterilization procedure and transparency to radio waves, compatibility with reinforcing agents, PEEK is considered as best alternative material to titanium in constructing implant abutments.^{31,39,40,41}

A study by Rea et al³⁵ evaluated the marginal soft and hard tissue healing at titanium and PEEK healing abutments over a 4 month period which shows that

when using PEEK as healing abutments the risk for marginal bone loss and soft tissue recession during healing period is not increased.³⁵

Stawarczyk et al⁴⁵ suggested PEEK in the fabrication of fixed partial denture. Hahnel et al¹⁹ investigated the formation of biofilms on different implant abutment materials and found that even though PEEK has high surface free energy than other abutment materials, the bio-film formation on the surface of PEEK is not higher than the zirconia and titanium. He suggested PEEK abutments to be used as a definite abutment material.⁴⁵

Since the abrasive resistance of PEEK is also excellent when compared to other metals. In this study, we used pre-machined PEEK abutments connected with titanium implants and compared with a group that contains premachined titanium abutments connected to titanium implants. To evaluate the 1 year simulation of clinical situation indicating the mastication, the abutments were cyclically loaded and analysed the effect of whether there is plastic deformation and wear when two different materials were connected.^{31,33,35,39,45,50}

In light of the above the aim of the present study was to comparatively evaluate the effect of cyclic loading on implant abutment interface of two different materials. The hypothesis for the present study was that, since the elastic modulus of PEEK is low there will be more wear in the PEEK abutment when compared with the titanium abutments. Brodbeck et al examined the wear effects

of dynamically loaded external connection titanium abutment with loose ceramic abutments and found that wear does occur between the components.²²

The methodology employed in this present study was able to quantify the wear at the implant abutment interface. Sterile titanium dental implants of the same dimension with an internal hexagon design were employed for standardization of the implant fixtures. The internal hexagonal connection system was selected because of its following advantages: ease in abutment connection, suitability for one-stage implant installation and single tooth restoration, higher stability and restoration to lateral loads due to lower center of rotation and better stress distribution than external hexagon implant connection systems.

Pre-machined straight abutments were selected for both the test groups simulating the clinical situation of maxillary anterior teeth. Premachined titanium straight abutments were chosen for Group I test samples (n=10). Premachined PEEK straight abutments were selected for Group II test samples (n=10). Implant abutment assembly positioning was standardized using dental surveyor. Auto polymerizing methyl methacrylate resin was used for securing the implants. The entire implant was submerged except for 1mm of the crest module to allow easy visualization.

A cement retained maxillary central incisor restoration cast with Ni-Cr alloy fabricated with an over-contoured cingulum area was done to accommodate the stylus of the cyclic loading apparatus.^{14,23}

Prior to cyclic loading all the abutments were connected to implants and the mid labial point was marked in both the abutment and in the resin block, which helps for reorientation. Then all the abutments were disconnected and analyzed for surface properties at the mid labial point which was chosen on the implant abutment interface area that is 90° from the marked point on abutment measuring the roughness of each abutment surface on the implant abutment interface would contribute to understand the mechanism of wear. Klotz et al²² stated that differences in the mechanical properties and designs could lead to wear at the interface. The quantitative measurements were made using SEM images. So, for analysis Surface Profilometry, Scanning Electron Microscopy and Energy Dispersive X-ray Spectrophotometry were carried out. These values were designated as pre cyclic loading surface roughness values namely Pre-Ra value₁ and Pre-Ra Value₂ for Group I and II test samples respectively. Then the abutments were connected to implants with 35 Ncm torque value.²² Then the Ni-Cr cast restorations were cemented.

A cyclic loading test was performed to simulate the component in function which permitted the analysis of wear on implant abutment interface of two

different abutment materials with the custom made cyclic loading machine. A cyclic load between 0 to 200N was applied at a loading rate 2Hz to simulate the force acting on maxillary anterior teeth. Loading done simulated 1 year of clinical loading based on previous literature on cyclic loading study.^{14,23}

The forces applied were at 30° inclination to the crown to simulate the functional stresses along the central incisor root angulations. To achieve this non-axial loading force for maxillary anterior region between 30°-40° angulations, a custom made positioning jig was used in the present study. Following cyclic loading each test sample was subjected to visual and tactile inspection for any deformation, decementation and abutment rotation or loosening as recommended in the previous studies. The restorations were decemented.

After cyclic loading quantitative and qualitative analysis were carried out for the samples of both the Groups. The post cyclic loading surface roughness values were measured and designated as Post-Ra Value₁ and Post- Ra Value₂ respectively for Group I and Group II samples. Further the mean Surface Roughness value Difference (Ra Value D) was obtained for both the test groups to assess the rate of wear. The data was analysed statistically using SPSS Software (version 20.0).

The mean pre-cyclic loading and post cyclic loading surface roughness values for Group I test samples (Pre-machined Titanium straight abutments) were

0.422 μm and 0.495 μm respectively and their mean surface roughness difference was -0.073 μm (Tables I,II and III respectively). In the present study, (Ra Value) the surface roughness value which indicates the wear rate following cyclic loading demonstrated that Group I test samples had exhibited higher surface roughness value in post cyclic loading compared to pre-cyclic loading and the difference (P value is 0.140) is statistically insignificant.

Klotz et al had mentioned in a study, that titanium implant connected to titanium abutment showed lesser wear rate compared to zirconia abutment because the interfacing materials had similar properties. The results of the present study also in line with Klotz et al's observation that titanium abutment had exhibited lesser wear rate.

The mean pre-cyclic loading and post cyclic loading surface roughness values for Group II test samples (Pre-machined PEEK straight abutments) were 0.232 μm and 0.233 μm . The mean Surface roughness difference value (Ra value D_2) of Group II test samples (Pre-machined PEEK straight abutments) was -0.0004 μm (Tables IV, V and VI respectively).

The Surface Roughness values between the two groups were compared. Surface roughness difference is the difference between pre-cyclic loading surface roughness value and the post cyclic loading surface roughness value which was calculated to assess the rate of wear. On comparison using Independent 't' test, it

was found that the mean difference values of pre and post- cyclic loading Surface roughness (Ra value) of Group I (Pre-machined Titanium straight abutments) (-0.073 μm) lower than the Group II test samples (Pre-machined PEEK straight abutments) (-0.0004 μm) and this was found to be statistically insignificant (p value is 0.272). The comparison of effect of cyclic loading on implant abutment interface between two different abutment materials was statistically insignificant. (Table IX) The result of the present study is in line with the study done by Almeida et al⁴ on comparative analysis of the wear of titanium/titanium and titanium/zirconia interfaces in implant/abutment assemblies after thermocycling and mechanical loading showed that there was no significant wear in simulating 5 years loading.⁴

The qualitative observations were made using SEM images. SEM micrographs taken before and after cyclic loading at 30x, 200x, 500x, 1000x shows patterns of wear in both the titanium and PEEK. At high magnification, the intensity and size of the wear could be seen. SEM micrograph of Group I test sample before cyclic loading revealed patchy irregularities and presence of voids under 500x and at 1000x, it appeared as sparsely distributed voids which indicating the rough surface. SEM micrograph of Group I test sample after cyclic loading revealed micro irregularities and diminution of voids under 500x and at 1000x, it appeared as sparsely distributed diminished voids indicating higher wear rate compared to pre cyclic loading. SEM micrograph of Group II test sample

before cyclic loading revealed micro striated irregularities under 500x and at 1000x, it appeared as sparsely distributed striations indicating smoother surface. SEM micrograph of Group II test sample after cyclic loading revealed increased micro striated irregularities under 500x and at 1000x it appeared as sparsely distributed striations indicating changes in surface topography which exhibits slightly higher wear compared to pre loading. EDS results of Titanium abutment before loading indicates the presence of 100% Titanium and after loading indicates the presence of 83.94% Titanium. EDS results of PEEK before loading indicates the presence of 100% Carbon and after loading indicates the presence of 66.04% Carbon. The percentage of depletion of Titanium from the Titanium abutments is less compared to percentage of depletion of PEEK from PEEK abutment which indicates lesser wear rate of Titanium abutment when compared to PEEK abutment.

The results obtained from quantitative and qualitative analysis coincides with each other and showed that wear was observed in both Group I and Group II test samples. Group II (PEEK abutment) test samples showed more wear when compared to Group I (Titanium abutment) test samples which might be due to difference in mechanical properties of implant abutment assembly in Group II. But the differences in wear for both the Groups were statistically insignificant.

Within the limitations of the present study, the results revealed PEEK could also be used as definite abutment. Thus the hypothesis was rejected as the premachined PEEK straight abutment shows wear rate close to premachined Titanium straight abutments.

The present study had some limitations. The duration of the cyclic loading was only one year simulation performed under dry condition and only pre-machined abutments were used. A longer loading period may affect the stability of implant abutment interface. The force employed here in this study is 200N only and the wear may vary with varying degree of force. Wear of the abutment assessed only at mid labial point and simulated only the maxillary anterior teeth. Presence of oral fluids may also impact the result differently. Parameters such as microbial leakage and fatigue testing may affect the interface differently.

Further studies needed to understand the influence of longer periods with larger sample size simulating in vivo conditions are recommended to add merit to the findings obtained with the present study.

CONCLUSION

The following conclusions were drawn based on the results obtained in the present in vitro study which was conducted to comparatively evaluate the wear resistance of two different implant abutment materials namely premachined Titanium straight abutment (Group I) and premachined PEEK straight abutment (Group II) after cyclic loading.

1. The mean Pre-cyclic loading Surface roughness value (Pre Ra value) of Group I test samples obtained by 3D Surface Profilometry was found to be 0.422 μm .
2. The mean Post-cyclic loading Surface roughness value (Post Ra value) of Group I test samples obtained by 3D Surface Profilometry was found to be 0.495 μm .
3. The mean Surface roughness difference value (Ra value D_1) between Pre cyclic and Post- cyclic loading of Group I test samples was found to be -0.073 μm .
4. The mean Pre-cyclic loading Surface roughness value (Pre Ra value) of Group II test samples obtained by 3D Surface Profilometry was found to be 0.232 μm .
5. The mean Post-cyclic loading Surface roughness value (Post Ra value) of Group II test samples obtained by 3D Surface Profilometry was found to be 0.233 μm .

6. The mean Surface roughness difference value (Ra value D_2) between pre cyclic and post cyclic loading of Group II test samples was found to be $-0.0004 \mu\text{m}$.
7. On comparison between the mean pre-cyclic loading ($0.422 \mu\text{m}$) and post cyclic loading ($0.495 \mu\text{m}$) surface roughness values for Group I test samples, the post-cyclic loading value was found to be higher which is statistically insignificant (P value is 0.140).
8. On comparison between the mean pre-cyclic loading ($0.232 \mu\text{m}$) and post cyclic loading ($0.233 \mu\text{m}$) surface roughness values for Group II test samples, the post cyclic loading value was found to be slightly higher which is statistically insignificant (P value is 0.976).
9. On comparison using Independent 't' test, it was found that the mean difference values of pre and post- cyclic loading Surface roughness values (Ra value) of Group I ($-0.073 \mu\text{m}$) was lower than the Group II test samples ($-0.0004 \mu\text{m}$) and this was found to be statistically insignificant. (p value is 0.272).
10. 3D Surface texture photomicrographs revealed that both Group I and Group II had exhibited rough surface after cyclic loading. Group II exhibited more rougher surface compared to Group I after cyclic loading. These observations corroborates with the quantitative analysis done with 3D Surface Profilometry.

11. SEM micrograph of Group I test sample before cyclic loading under 500x revealed patchy irregularities and presence of voids and under 1000x, the voids appeared as sparsely distributed, which indicates the rough surface.
12. SEM micrograph of Group I test sample after cyclic loading under 500x revealed micro irregularities and diminution of voids and under 1000x, the voids appeared diminished and sparsely distributed, indicating more wear in the rough surface.
13. SEM micrograph of Group II test sample before cyclic loading under 500x revealed micro striated irregularities and under 1000x, the irregularities appeared as sparsely distributed striations, indicating smoother surface.
14. SEM micrograph of Group II test sample after cyclic loading under 500x revealed increased micro striated irregularities and under 1000x, the irregularities appeared as sparsely distributed striations, indicating rough surface.
15. The SEM observations made with both groups before and after cyclic loading revealed wear of the tested samples and more rougher surface with Group II which correlates with higher surface roughness value obtained by 3D Surface Profilometry.
16. EDS results of Titanium abutment before loading indicates the presence of 100% Titanium and after loading indicates the presence of 16.36% Aluminium and 83.94% Titanium. The decrease in the percentage of Titanium after cyclic loading indicates the wear of Titanium.

17. EDS results of PEEK before loading indicates the presence of 100% Carbon and after loading indicates the presence of 66.04% Carbon and 33.96% Oxygen. The decrease in the percentage of carbon after cyclic loading indicates the wear of PEEK.
18. EDS results revealed that the percentage of wear of Titanium (16.36%) is lesser than that of PEEK (33.96%).
19. The lesser the surface roughness value of Titanium abutments obtained after cyclic loading determined by 3D Surface Profilometry corroborates with lesser rough surface observed by SEM and lesser percentage of depletion of Titanium by EDS revealed that the wear resistance of Titanium abutment is higher than that of PEEK abutments but the difference between these two implant abutment materials does not show any statistical significance.

SUMMARY

The Present in vitro study was conducted to comparatively evaluate the wear resistance between two different implant abutment materials after cyclic loading.

Twenty titanium implants (standard platform) of 4.2 mm × 10 mm were selected. Ten implants were used to connect the Titanium abutments (Group I) and other ten were used to connect the PEEK abutments(Group II). The implant abutment assemblies were positioned in the stainless steel block with the help of surveyor and secured with auto polymerizing acrylic resin. Qualitative and quantitative assessment of abutments at the implant abutment interface for both the groups were evaluated using Surface profilometry, Scanning Electron Microscopy and Energy Dispersive X-ray Spectrophotometry.

The cement retained Nickel chromium cast crowns were fabricated for all the abutments of both the groups. Abutments were torqued to 35 Ncm to their respective implants and crowns were cemented. Cyclic loading with loads up to 200N simulating the masticatory forces in the anterior maxilla region was done at 30° angulation using customized cyclic loading machine. After loading for 5,50,000 cycles simulating 1 year. Crowns were removed and abutments were disconnected from the implants.

The post- cyclic loading values at the implant abutment interface were evaluated for surface roughness (Ra) values using Surface profilometer, Scanning Electron Microscope and Energy Dispersive X-ray Spectrophotometer. The Surface Roughness difference was calculated from the pre-cyclic and post-cyclic loading Surface Roughness values for each test

sample respectively for both Groups I and II. The results obtained were tabulated and statistically analysed.

The mean pre cyclic loading and post cyclic loading surface roughness value for Group I test samples were found to be 0.422 μm and 0.495 μm respectively and their difference was -0.073 μm . The mean pre cyclic loading and post cyclic loading surface roughness value for Group II test samples were found to be 0.232 μm and 0.233 μm respectively and their difference was -0.0004 μm . On statistical comparison the differences in the Surface roughness values for both the groups were statistically insignificant.

The quantitative analysis of Group I and Group II test samples obtained by 3D Surface Profilometry had revealed that the Group I samples have higher wear resistance compared to Group II samples but the difference in wear resistance is statistically insignificant. The results of the qualitative analysis obtained from SEM and EDS of the test samples corroborates with the quantitative analysis.

Within the limitations of the present study, the surface roughness values before and after cyclic loading of two different abutment materials revealed that the wear resistance of titanium abutments is more than that PEEK abutments but the difference in the wear resistance is statistically insignificant.

The present study had revealed statistically insignificant wear among the two implant abutment materials after cyclic loading. Hence, PEEK could prove to be a viable alternative to titanium to use as an implant abutment depending on the clinical condition of the patients.

BIBLIOGRAPHY

1. **Albrektsson T, Branemark PI, Hansson HA, Lindstrom J.** Osseointegrated titanium implants: requirements for ensuring a long-lasting, direct bone-to-implant anchorage in man. *Acta Orthop Scand.* 1981;52:155–170.
2. **Al-Jadaa A, Attin T, Peltomäki T, Heumann C, Schmidlin PR.** Impact of dynamic loading on the implant-abutment interface using gas enhanced permeation test In Vitro. *Open Dent J*, 2015;9:112-119.
3. **Almeida, P. J., Silva, C. L., Alves, J. L., Silva, F. S., Martins, R. C., & Sampaio Fernandes, J. (2016).** Comparative analysis of the wear of titanium/titanium and titanium/zirconia interfaces in implant/abutment assemblies after thermocycling and mechanical loading. *Revista Portuguesa de Estomatologia, Medicina Dentária e Cirurgia Maxilofacial*, 57(4), 207–214.
4. **Alqahtani F and Flinton R,** Postfatigue fracture resistance of modified prefabricated zirconia implant abutments. *J Prosthet Dent* 2014: Aug ; 112(2):299-305
5. **Apicella D, Veltri M, Chieffi N, Polimeni A, Giovannetti A, Ferrari M.** Implant adaptation of stock abutments versus CAD/CAM abutments: a radiographic and scanning electron microscopy study *Annali di Stomatologia* 2010;1(3-4):9-13.
6. **Balik A, Karatas MO, Keskin H.** Effects of different abutment connection designs on the stress distribution around five different implants:

a 3-dimensional finite element analysis. J Oral Implantol. 2012 Sep;38 Spec No:491-6.

7. **Binon PP.** Implants and Components: Entering and New Millenium. Quintessence Publishing 2000;15:76-95.
8. **Bishti S ,Strub RJ & Wael Att.** Effect of the implant–abutment interface on peri-implant tissues:A systematic review. Acta OdontologicaScandinavica, 2014; 72: 13–25.
9. **Chun HJ, Yeo IS, Lee JH, Kim SK, Heo SJ, Koak JY, Han JS, Lee SJ.** Fracture strength study of internally connected zirconia abutments reinforced with titanium inserts. Int J Oral Maxillofac Implants. 2015 Mar-Apr;30(2):346-50.
10. **de Carvalho GA, Franco AB, Kreve S, Ramos EV, Dias SC, do Amaral FL.** Polyether ether ketone in protocol bars: Mechanical behavior of three designs. J Int Oral Health 2017;9:202 - 6.
11. **Dr. Prabhu, R. and Dr. Sudheer.** “Review on implant - Abutment interface”, *International Journal of Current Research*, 2017, 9, (10), 58701-58704.
12. **Dr. Unjum Bashir, Dr. Manas Gupta, Dr.Ravish Ahuja.** Implant systems. International Journal of Applied Dental Sciences 2016, Vol. 2 Issue 2, Part A.
13. **El Houssiney AG, Zhang H, Song J, Ji P, Wang L, Yang S.** Influence of implant location on the clinical outcomes of implant abutments: a

systematic review and meta-analysis. Clinical, Cosmetic and Investigational Dentistry 2018;Feb 26;10:19-35

14. **Elsayed A, Wille S, Al-Akhali M, Kern M.** Effect of fatigue loading on the fracture strength and failure mode of lithium disilicate and zirconia implant abutments. *Clin Oral Impl Res.* 2017;00:1–8.
15. **De Avila ED, Vergani CE, FransicoA, Mollo Junior FA, Junior MJ, Shi W, Lux R.**Effect of titanium and zirconia dental implant abutments on a cultivable polymicrobial saliva community.J Prosthet Dent 2017 Oct;118(4):481-487.
16. **Foong JK, Judge RB, Palamara JE, Swain MV.** Fracture resistance of titanium and zirconia abutments: an in vitro study. J Prosthet Dent. 2013 May;109(5):304-12.
17. **Fujiwara CA, Filho OM, Oliveira NTC, Queiroz TP, Abila MS, Pardini LC.** Assessment of the interface between implant and abutments of five systems by scanning electronic microscopy. Osseointe 2009;2(1):60-93
18. **Gil FJ, Herrero-Climent M, Lúzaró P, Rios JV.** Implant-abutment connections: influence of the design on the microgap and their fatigue and fracture behaviour of dental implants. J Mater Sci: Mater: Med 2014.Jul; 25(7):1825-30.
19. **Hahnel S, Wieser A, Lang R, Rosentritt M.** Biofilm formation on the surface of modern implant abutment materials. Clin. Oral Impl. Res. 00, 2014; 1–5.
20. **Kaleli N., Sarac D., Kulunk S., Ozturk O.** Effect of different restorative crown and customized abutment materials on stress distribution in single

implants and peripheral bone: A three-dimensional finite element analysis study. *Journal of Prosthetic Dentistry*, Volume 119 , Issue 3 , 437 – 445.

21. **Kern, Matthias & Lehmann, Frank. (2012).** Influence of surface conditioning on bonding to polyetheretherketon (PEEK). *Dental materials : official publication of the Academy of Dental Materials*. 28. 1280-3. 10.1016/j.dental.2012.09.010.
22. **Kim JS, Kim HJ, Chung CH, Back DH.** Fit of fixture/abutment screw interfaces of internal connection implant system J *Korean AcadProsthodont*. 2005; 43(3): 338-51.
23. **Klotz MW, Taylor TD, Goldberg AJ.** Wear at the titanium–zirconia implant–abutment interface: a pilot study. *the international journal of oral and maxillofacial implants* 2011;26:970–5.
24. **Koutouzis T, Richardson J, Lundgren T,** ComparativeSoft and Hard Tissue Responses to Titanium and Polymer Healing Abutments. *Journal of Oral Implantology*, Volume XXXVII/2011.
25. **Kurt A, Isik-Ozkol G.** Conventional methods for selecting form, size, and color of maxillary anterior teeth: Review ofthe literature. *Eur J Prosthodont*2015;3:57-63.
26. **Lee BA, Kim BH, Kweon HHI, Kim YT.** The prosthetic abutment height can affect marginal bone loss around dental implants. *Clin Implant Dent Relat Res*. 2018;1–7.
27. **Meuhlemann S, Truninger TC, Stawarczyk B, H€ammerle CHF, Sailer I.** Bending moments of zirconia and titanium implant abutments

supporting all-ceramic crowns after aging. Clin. Oral Impl. Res. 25, 2014, 74–81.

28. **Mishra SK, Chowdhary R, Hazari P.** Polyetheretherketone implants: Can they replace titanium in future. Eur J Prosthodont 2016;4:41 - 2.
29. **Moraschini V, L. A. da C. Poubel, Ferreira FV, E. dos S. Barboza P:** Evaluation of survival and success rates of dental implants reported in longitudinal studies with a follow-up period of at least 10 years: a systematic review. Int. J. Oral Maxillofac. Surg. 2014.
30. **Muley N. Prithvi DR, Gupta V.** Evolution of external and internal implant to abutment connection. Int J Oral Implantol Clin Res 2012;3(3):122-129.
31. **Najeeb S,** Applications of polyetheretherketone (PEEK) in oral implantology and prosthodontics. J Prosthodont Res 2016 Jan ;60(1):12-9
32. **Newmann EAF, Villar CC and Franca EMG.** Fracture resistance of abutment screws made of titanium, polyetheretherketone, and carbon fiber-reinforced polyetheretherketone. Braz Oral Res., (São Paulo) 2014;28(1):1-5.
33. **Rae, P.J. & Brown, Eric &Orler, E.B.. (2007).** The Mechanical Properties of Poly(Ether-Ether-Ketone) (PEEK) with Emphasis on the Large Compressive Strain Response. Polymer. 48. 598-615. 10.1016/j.polymer.2006.11.032.

34. **Rahmitasari F, Ishida Y, Kurahashi K, Matsuda T, Watanabe M, Ichikawa T.** PEEK with Reinforced Materials and Modifications for Dental Implant Applications. *Dent. J.* 2017, 5, 35.
35. **Rea M, Ricci S, Ghensi P, Lang NP, Botticelli D, Soldini C.** Marginal healing using Polyetheretherketone (PEEK) as healing abutments: an experimental study in dogs. *Clin. Oral Impl. Res.* 00, 2016, 1–5
36. **Rho JY, Ashman RB, Turner CH.** Young's modulus of trabecular and cortical bone material: ultrasonic and microtensile measurements. *Journal of Biomechanics* 1993;26:111–9.
37. **Ribeiro CG, Maia ML, Scherrer SS, Cardoso AC, Wiskott HW.** Resistance of three implant-abutment interfaces to fatigue testing. *J Appl Oral Sci* 2011;19(4):413-20.
38. **Saidin S, Abdul Kadir MR, Sulaiman E, Abu Kasim NH.** Effects of different implant–abutment connections on micromotion and stress distribution: prediction of microgap formation. *Journal of Dentistry* 2012;40:467–74.
39. **Sailer I, Philipp A, Zembic A, Pjetursson BE, Ha'immerle CHF, Zwahlen M.** A systematic review of the performance of ceramic and metal implant abutments supporting fixed implant reconstructions. *Clin. Oral Impl. Res.* 20 (Suppl. 4), 2009; 4–31.
40. **Santing HJ, Henny J. A. Meijer, Raghoobar GM, Özcan M.** Fracture Strength and Failure Mode of Maxillary Implant-Supported Provisional Single Crowns: A Comparison of Composite Resin Crowns Fabricated

Directly Over PEEK Abutments and Solid Titanium Abutments. Clin Implant Dent Relat Res.2012 Dec;14(6):882-889.

41. **Sawase T, Wennerberg A, Hallgren C, Albrektsson T, Baba K.** Chemical and topographical surface analysis of five different implant abutments. Clin Oral Impl Res 2000; 11: 44–50.
42. **Scheller H, Urgell JP, Kultje C, et al:** A 5-year multicenter study on implant-supported single crown restorations. Int J Oral Maxillofac Implants 1998;13:212-218.
43. **Schwitalla DA, Zimmermann T, Spintig T, Abou-Emara M, Lackmann J, Müller WD and Houshmand A.** Maximum Insertion Torque of a Novel Implant-Abutment- Interface Design for PEEK Dental Implants, Journal of the Mechanical Behavior of Biomedical Materials; 2018, Jan;77:85-89
44. **Seaman S, Kerezoudis P, Bydon M, Torner JC, Hitchon PW.** Titanium vs. polyetheretherketone (PEEK) interbody fusion: Meta-analysis and review of the literature. J Clin Neurosci 2017 Oct;44:23-29.
45. **Stawarczyk, Bogna; Jordan, Peter; Schmidlin, Patrick R; Roos, Malgorzata; Eichberger, Marlis; Gernet, Wolfgang; Keul, Christine.** PEEK surface treatment effects on tensile bond strength to veneering resins. Journal of Prosthetic Dentistry, 2014, 112(5):1278-1288.
46. **Stimmelmayer M, Sagerer S, Erdelt K, Beuer F.** In vitro fatigue and fracture strength testing of one-piece zirconia implant abutments and zirconia implant abutments connected to titanium cores.Int J Oral Maxillofac Implants. 2013 Mar-Apr;28(2):488-93.

47. **Steinebrunner L, Wolfart S, Ludwig K, Kern M.** Implant–abutment interface design affects fatigue and fracture strength of implants. *Clinical Oral Implants Research* 2008;19:1276–84.
48. **Tetelman ED and Babbush CA,** A New Transitional Abutment for Immediate Aesthetics and Function. *Implant Dent* 2008;17:51–58.
49. **Truninger TC, Stawarczyk B, Leutert CR, Sailer TR, Ha`mmerle CHF, Sailer I.** Bending moments of zirconia and titanium abutments with internal and external implant–abutment connections after aging and chewing simulation. *Clin. Oral Impl. Res.* 23, 2012; 12–18.
50. **Turner J, Menary Gand Martin P.** Biaxial Deformation Behaviour of Poly-Ether-Ether-Ketone. *AIP Conf. Proc.* 1960, 120021-1–120021-6.
51. **Val, J.E.M.S., G´omez-Moreno, G., Mart´inez, C.P.-A., Fern´andez, M.P.R., Mar´in, J.M.G., Gehrke, S.A., Calvo-Guirado, J.L.** Peri-implant tissue behavior around non-titanium material: Experimental study in dogs, *Annals of Anatomy* . Vol 206, July 2016, Pages 104-109.
52. **Vidigal Jr GM, Novaes Jr AB, Chevitaese 0, Avillez RR, an M.** Evaluation of the implant-abutment connection interface using scanning electron microscopy. *Braz Dent J.* 1995;60):17-23.
53. **Wang CF, Huang HL, Lin DJ, Shen YW, Fuh LJ and Hsu JT .** Comparisons of maximum deformation and failure forces at the implant–abutment interface of titanium implants between titanium-alloy and zirconia abutments with two levels of marginal bone loss. *BioMedical Engineering OnLine* 2013 12:45.

54. **Watkin A, Kerstein RB.** Improving darkened anterior peri-implant tissue color with zirconia custom implant abutments. *Compend Contin Educ Dent* 2008;29:238–240,242.
55. **Yilmaz B, Salaita LG, Seidt JD, Clelland NL, Mc Glumphy EA.** Load to failure of different titanium abutments for an internal hexagon implant. *J Prosthet Dent.* 2015 Oct;114(4):513-6.
56. **Yuzugullu B, Avci M.** The implant–abutment interface of alumina and zirconia abutments. *Clinical Implant Dentistry and Related Research* 2008;10:113–21.

ANNEXURE VIII

PLAGIARISM REPORT

URKUND

Urkund Analysis Result

Analysed Document: plagiarism.pdf (D47625633)
Submitted: 2/5/2019 6:11:00 PM
Submitted By: mnamuthu121@gmail.com
Significance: 4 %

Sources included in the report:

<https://www.readbyqxmd.com/journal/30708/11>
<https://www.ncbi.nlm.nih.gov/pubmed/27080305>
<http://repository-tnmgrmu.ac.in/5504/>
<https://www.sciencedirect.com/science/article/pii/S1883195815000997>
http://repository-tnmgrmu.ac.in/10005/1/240102318ashwini_sukanya.pdf

Instances where selected sources appear: